Lymphoid differentiation of hematopoietic stem cells requires efficient Cxcr4 desensitization

Christelle Freitas,[1] Monika Wittner,[2] Julie Nguyen,[1] Vincent Rondeau,[1] Vincent Biajoux,[1] Marie-Laure Aknin,[3] Françoise Gaudin,[1,3] Sarah Beaussant-Cohen,[4] Yves Bertrand,[5] Christine Bellanné-Chantelot,[6] Jean Donadieu,[7] Françoise Bachelerie,[1] Marion Espéli,[1] Ali Dalloul,[1] Fawzia Louache,[2]* and Karl Balabanian[1]*

[1]Inflammation Chemokines and Immunopathology, Institut National de la Santé et de la Recherche Medicale (INSERM), Faculté de Médecine, Université Paris-Sud, Université Paris-Saclay, Clamart, France
[2]INSERM UMR_S1170, Institut Gustave Roussy, CNRS GDR 3697 MicroNiT, Université Paris-Sud, Université Paris-Saclay, Villejuif, France
[3]Institut Paris-Saclay d'Innovation Thérapeutique, UMS IPSIT-US31-UMS3679, Chatenay-Malabry, France
[4]Service d'Hémato-Oncologie Pédiatrique, CHU Jean Minjoz, Université de Franche-Comté, Besançon, France
[5]Service d'Hémato-Oncologie Pédiatrique, Hospices Civils de Lyon, Université Claude Bernard Lyon I, Lyon, France
[6]AP-HP, Hôpital Pitié-Salpêtrière, Département de Génétique, Université Pierre et Marie Curie, Paris, France
[7]AP-HP, Registre Français des Neutropénies Chroniques Sévères, Centre de référence des Déficits Immunitaires Héréditaires, Service d'Hémato-Oncologie Pédiatrique, Hôpital Trousseau, Paris, France

The CXCL12/CXCR4 signaling exerts a dominant role in promoting hematopoietic stem and progenitor cell (HSPC) retention and quiescence in bone marrow. Gain-of-function *CXCR4* mutations that affect homologous desensitization of the receptor have been reported in the WHIM Syndrome (WS), a rare immunodeficiency characterized by lymphopenia. The mechanisms underpinning this remain obscure. Using a mouse model with a naturally occurring WS-linked gain-of-function *Cxcr4* mutation, we explored the possibility that the lymphopenia in WS arises from defects at the HSPC level. We reported that Cxcr4 desensitization is required for quiescence/cycling balance of murine short-term hematopoietic stem cells and their differentiation into multipotent and downstream lymphoid-biased progenitors. Alteration in Cxcr4 desensitization resulted in decrease of circulating HSPCs in five patients with WS. This was also evidenced in WS mice and mirrored by accumulation of HSPCs in the spleen, where we observed enhanced extramedullary hematopoiesis. Therefore, efficient Cxcr4 desensitization is critical for lymphoid differentiation of HSPCs, and its impairment is a key mechanism underpinning the lymphopenia observed in mice and likely in WS patients.

INTRODUCTION

CXCR4 is a broadly expressed G-protein–coupled receptor whose activation by its natural ligand, the CXC α-chemokine stromal cell–derived factor 1 (SDF-1/CXCL12), is essential for fetal B cell lymphopoiesis and BM myelopoiesis (Nagasawa et al., 1996, 1998; Ma et al., 1998). In postnatal life, CXCR4 mediates the engraftment, retention, and multilineage differentiation of hematopoietic stem and progenitor cells (HSPCs) in various CXCL12-expressing BM niches by regulating their migration, survival, and quiescence (Peled et al., 1999; Foudi et al., 2006; Nie et al., 2008; Karpova and Bonig, 2015; Cordeiro Gomes et al., 2016). This signaling axis is also involved at different stages in the production and distribution of B, T, and myeloid cells in lymphoid organs (LOs) and peripheral blood (Nagasawa et al., 1996; Kawabata et al., 1999; Onai et al., 2000; Scimone et al., 2004; Eash et al., 2010). Our current understanding of the role of CXCR4 in lymphocyte biology is mostly based on data generated from mice deficient in *Cxcr4*, *Cxcr4*$^{-/-}$ chimeras, or conditional knockout mice in which *Cxcr4* was selectively inactivated in the B or T cell lineage (Nagasawa et al., 1996, 1998; Ma et al., 1998; Nie et al., 2008; Trampont et al., 2010; Tzeng et al., 2011). Recently, selective deletion of *Cxcl12* or *Cxcr4* in BM stroma has allowed the identification of specialized niches supporting the homeostasis of HSPCs and leukemia-initiating cell maintenance (Ding and Morrison, 2013; Pitt et al., 2015; Itkin et al., 2016).

CXCR4 desensitization and endocytosis regulate its signaling pathways and activities. Upon CXCL12 exposure,

Dr. Dalloul died on April 16, 2015.

*F. Louache and K. Balabanian contributed equally to this paper.

Correspondence to Karl Balabanian: karl.balabanian@u-psud.fr

Abbreviations used: 5-FU, 5-fluorouracil; BV, brilliant violet; CLP, common lymphoid progenitor; CMP, common myeloid progenitor; C-tail, carboxyl-terminal tail; DN, double negative; EMH, extramedullary hematopoiesis; ETP, early thymic progenitor; GMP, granulocyte-macrophage progenitor; HSC, hematopoietic stem cell; HSPC, hematopoietic stem and progenitor cell; LMPP, lymphoid-primed MPP; LO, lymphoid organ; LRC, label-retaining cell; LT-HSC, long-term HSC; MEP, megakaryocyte-erythroid progenitor; MPP, multipotent progenitor; pre–B cell, B cell precursor; pro–B cell, B cell progenitor; SLAM, signaling lymphocyte activation molecule; ST-HSC, short-term HSC; WS, WHIM syndrome.

The Rockefeller University Press $30.00
J. Exp. Med. 2017 Vol. 214 No. 7 2023–2040
https://doi.org/10.1084/jem.20160806

β-arrestins are recruited to the carboxyl-terminal tail (C-tail) domain of the receptor, precluding further G-protein activation (i.e., desensitization) and leading to receptor internalization. Moreover, CXCR4 internalization is associated with HSPC entry into the circulation (Christopher et al., 2009). In line with this, in normal human circulating $CD34^+$ hematopoietic progenitor cells, a large proportion of CXCR4 is sequestered intracellularly as a consequence of constitutive internalization (Zhang et al., 2004). This suggests that the intracellular trafficking of CXCR4 is a highly regulated process and raises the question of its role in the biological properties of HSPCs. Dysregulated CXCR4 inactivation and internalization might be expected to impair HSPC differentiation, recirculation or trafficking, resulting in cytopenia and immunodeficiency.

The majority of cases of the rare primary immunodeficiency WHIM (warts, hypogammaglobulinemia, infections, and myelokathexis) syndrome (WS) has been linked to inherited autosomal-dominant gain-of-function mutations in *CXCR4* (Kawai and Malech, 2009; Dotta et al., 2011). This results in the distal truncation of the C-tail of CXCR4 and a desensitization- and internalization-resistant receptor in response to CXCL12 (Hernandez et al., 2003; Balabanian et al., 2005). Similar dysfunctions of CXCR4 were observed in leukocytes from some patients with WS but carrying a wild-type *CXCR4* coding sequence ($WHIM^{WT}$; Balabanian et al., 2005, 2008). Patients exhibit severe, chronic pan-leukopenia, with naive T cells and mature recirculating B cells most affected (Gulino et al., 2004). Given that CXCR4 is widely expressed on nonhematopoietic cells and virtually all leukocytes at multiple stages of development, one possibility could be that WS-associated peripheral blood leukopenia is a consequence of skewed production, differentiation, or distribution of leukocytes related to altered CXCR4-mediated signaling. The recent discovery by McDermott et al. (2015) of a chromothriptic cure of WS supports this hypothesis. They found deletions of one copy of chromosome 2, including the disease allele $CXCR4^{R334X}$, in a hematopoietic stem cell (HSC) of a patient who had spontaneously repopulated the myeloid but not the lymphoid lineage. This natural experiment suggests that WS-related neutropenia and monocytopenia stem from a hematopoietic defect.

Recently, we have been able to replicate the hematologic phenotype of WS using a knock-in $Cxcr4^{+/1013}$ mouse strain (+/1013) that harbors the WS-linked heterozygous $CXCR4^{S338X}$ mutation causing a distal truncation of the last 15 residues of the C-tail domain (Balabanian et al., 2012). Mutant mice displayed lymphocytes with enhanced migration to Cxcl12, phenocopied severe lymphopenia and failed to maintain antibody titers after immunization (Biajoux et al., 2016). First-line analyses of +/1013 mice suggested developmental defects at the B cell progenitor (pro–B cell)/B cell precursor (pre–B cell) stage in the BM and during the early double-negative (DN) stages of thymocyte maturation (Balabanian et al., 2012). However, whether impaired lymphopoiesis stems from an upstream cell-intrinsic hematopoietic defect remains to be established. Here, we took advantage of our relevant knock-in model and the access to blood samples from five WS patients to investigate the impact of CXCR4 desensitization on hematopoiesis and HSPC recirculation.

RESULTS

The reduction in early B/T cell progenitors is proportional to $Cxcr4^{1013}$ allelic dose

To determine how the gain-of-*Cxcr4*-function mutation impacts HSPC homeostasis (Fig. S1 A), global hematopoietic development was assessed in nonmanipulated $Cxcr4^{+/+}$ (WT) and +/1013 mice. To avoid interference by the WT allele, we also analyzed homozygous $Cxcr4^{1013/1013}$ (1013/1013) mice. There was a profound lymphopenia in mutant mice that affects predominantly naive ($CD3^+CD44^{-/low}CD62L^{high}$) T and immature ($B220^+IgM^{high}CD21^{low}$) B cells and follows a $Cxcr4^{1013}$ allele dose-dependent pattern (Fig. 1 A). Red blood cell and platelet counts, as well as hematocrit and hemoglobin levels, did not differ between WT and mutant mice (Table 1). We next performed detailed immunophenotyping of early lymphoid progenitors in primary LOs. In the BM, 1013/1013 mice exhibited earlier and more severe defects in B cell ontogeny than +/1013 mice, with reductions in both pro–B cells ($B220^+IgM^-CD43^+$) and pre–B cells ($B220^+IgM^-CD43^-$; Fig. 1 B). We also observed a clear $Cxcr4^{1013}$ allele dose-dependent increase in the proportion of apoptotic pro– and pre–B cells (Fig. 1 C). Numbers of developing T cells, including DN1–DN4 thymocytes, were also significantly reduced in a $Cxcr4^{1013}$ allele dose-dependent fashion (Fig. 1 D). Moreover, the number of early thymic progenitors (ETPs), defined as $Lin^-CD4^-CD8^-c\text{-}Kit^+CD44^{high}CD25^-$, was reduced in a $Cxcr4^{1013}$ allele dose-dependent manner (Fig. 1 E and Fig. S1 B).

To determine whether the reduction in early B/T cell progenitors and the circulating lymphopenia result from a lymphocyte-intrinsic defect or an alteration of the LO microenvironment, BM reconstitution experiments were performed (Fig. 1 G). BM cells from WT, +/1013, or 1013/1013 $CD45.2^+$ mice were transplanted into lethally irradiated WT $CD45.1^+$ recipients. Four months after reconstitution, there were significantly lower numbers of T and B cells in the blood of $Cxcr4^{1013}$-bearing BM-chimeric mice compared with WT chimeras (Fig. 1 H, left). Pro–B cells were substantially decreased in the BM of 1013/1013 engrafted mice, whereas ETPs were decreased in the thymus of both $Cxcr4^{1013}$-bearing BM-chimeric mice (Fig. 1 H, middle and right). We performed reverse chimeras in which $CD45.2^+$ WT and mutant mice were irradiated and reconstituted with WT $CD45.1^+$ BM (Fig. 2 A). The numbers of lymphocytes in peripheral blood, pro–B cells in BM, and ETP in thymus were comparable in all groups (Fig. 2 B). There was a decrease in the number of $CD11b^+Gr\text{-}1^+$ myeloid cells in the blood of mutant mice that followed a $Cxcr4^{1013}$ allele dose-dependent pattern (Fig. 1 F, left). This was mirrored

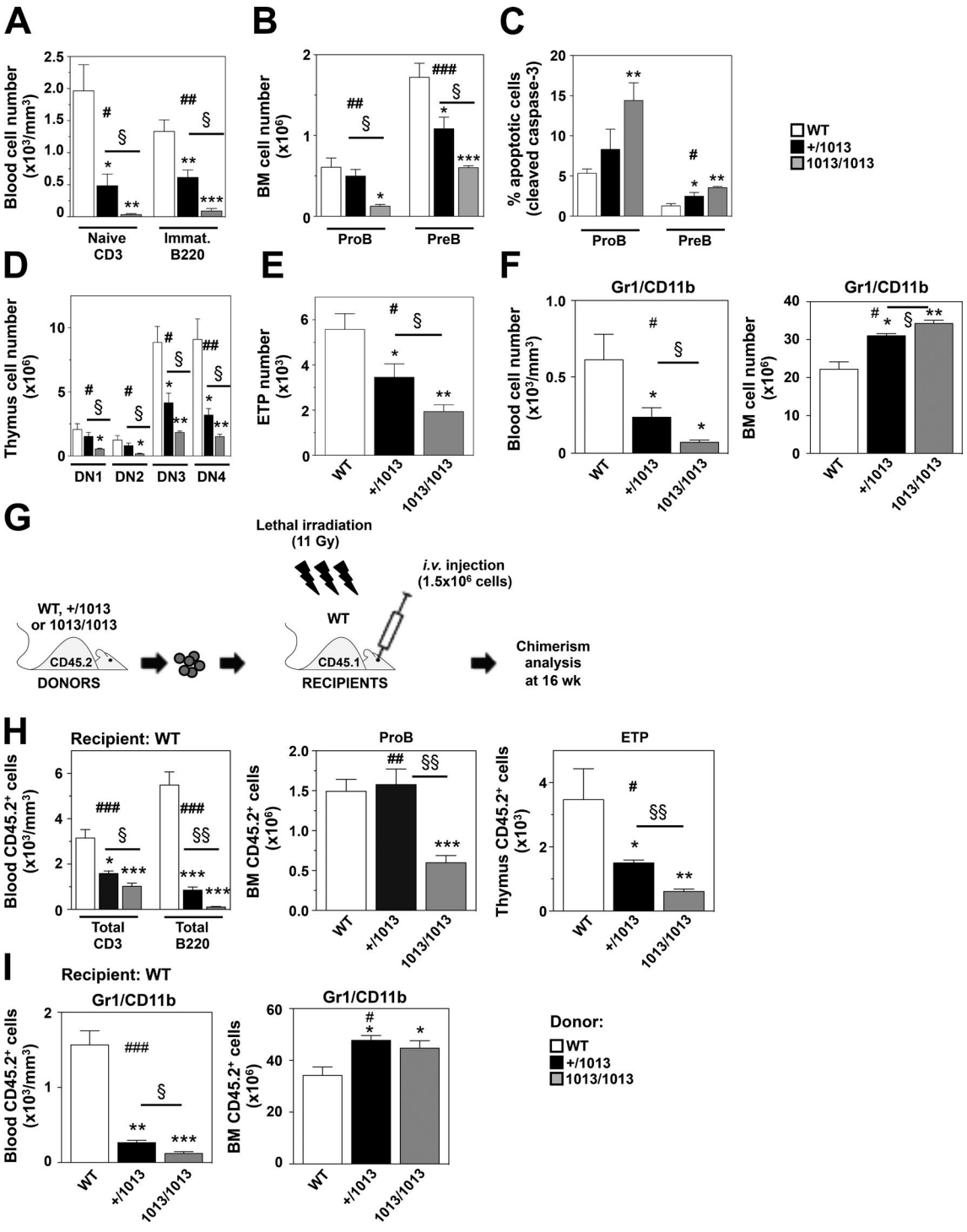

Figure 1. **Reduction in *Cxcr4*^{1013}-bearing early B and T cell progenitors involves cell-intrinsic defects.** (A) Absolute numbers of naive (CD44$^{-/low}$CD62L^{high}) CD3^{+} T cells and immature (Immat.; B220^{+}IgM^{high}CD21^{low}) B cells were determined by flow cytometry from blood samples of WT, *Cxcr4*$^{+/1013}$ (+/1013), and *Cxcr4*$^{1013/1013}$ (1013/1013) mice. Data are from three independent experiments with five to nine mice per group. (B) Absolute numbers of pro–B cells (B220^{+}IgM^{-}CD43^{+}) and pre–B cells (B220^{+}IgM^{-}CD43^{-}) were determined from two femurs. Data are from four independent experiments with seven mice per group. (C) Caspase-3 cleavage was used to detect the percentages of apoptotic BM pro– and pre–B cells. Data are from two independent experiments with six mice per group. (D and E) Total thymi were analyzed for numbers of DN stage 1 (DN1; CD4^{-}CD8^{-}CD44^{+}CD25^{-}), DN2 (CD44^{+}CD25^{+}), DN3 (CD44^{-}CD25^{+}), and DN4 (CD44^{-}CD25^{-}) cells (D) and for numbers of ETP (Lin^{-}CD4^{-}CD8^{-}c-Kit^{+}CD44^{high}CD25^{-}) cells (E). Data are from four independent experiments with seven mice per group. (F) Absolute numbers of myeloid cells (Gr1^{+}CD11b^{+}) were determined from blood and BM samples of WT and mutant

by an increase in myeloid cells in the BM (Fig. 1 F, right). Comparable findings were obtained in the blood and BM of *Cxcr4*^{1013}-bearing BM-chimeric mice compared with WT chimeras (Fig. 1 I). Reverse chimeras revealed no change in the number of myeloid cells in the blood and BM between all groups (Fig. 2 C). Thus, both the reduction in early T and B cell progenitors and the increase in mature myeloid cells in the BM of *Cxcr4*^{1013}-bearing mice result from a cell-intrinsic defect in Cxcr4-mediated signaling.

The pool of *Cxcr4*^{1013}-bearing lymphoid-committed progenitors is reduced in the BM

HSCs generate mature leukocytes via a succession of increasingly committed downstream progenitor cells (Doulatov et al., 2012). Thus, we quantified the pool of lymphoid-primed multipotent progenitors (MPPs [LMPPs];Lin$^-$c-Kit$^+$Sca-1$^+$ [LSK] Flt3^{high}CD34$^+$) and common lymphoid progenitors (CLPs; Lin$^-$c-Kit^{low}Sca-1^{low}Flt3$^+$CD127$^+$) in the BM of WT and mutant mice (Fig. S1, A and C; Ding and Morrison, 2013). There was a profound decrease in the number of LMPPs and CLPs in mutant mice (Fig. 3 A). BM chimeras were used to demonstrate that this decrease in lymphoid progenitors observed in *Cxcr4*^{1013}-bearing mice involved a cell-intrinsic defect (Fig. 3 C). In contrast to the reduction in LMPPs and CLPs, no changes in common myeloid progenitors (CMPs; Lin$^-$c-Kit$^+$Sca-1$^-$CD34$^+$CD16/32$^-$),granulocyte-macrophage progenitors (GMPs; Lin$^-$c-Kit$^+$Sca-1$^-$CD34$^+$CD16/32$^+$) and megakaryocyte-erythroid progenitors (MEPs; Lin$^-$c-Kit$^+$ Sca-1$^-$CD34$^-$CD16/32$^-$) could be detected (Fig. 3, B and C). These findings suggest a reduced capacity of *Cxcr4*^{1013}-bearing HSPCs to generate the earliest lymphoid progenitors while leaving their apparent ability to produce myeloid progenitors intact.

Loss of lymphoid potential occurs at the HSC-to-MPP transition in the absence of Cxcr4 desensitization in vitro

The major divergence of lymphoid and myeloid lineages occurs at the MPP stage (Fig. S1 A). To characterize the stage from which the lymphopoiesis process is impacted in mutant mice, we next assessed the pool of MPPs (LSK CD48$^-$CD150$^-$). Intriguingly, although the CMP pool was not affected in *Cxcr4*^{1013}-bearing mice, there was a *Cxcr4*^{1013} allele dose-dependent decrease in the number of MPPs in mutant mice (Fig. 3 A). MPPs defined as LSK Flt3$^+$CD34$^+$ (Hidalgo et al., 2012) were also decreased in the BM of mutant mice (not depicted). BM chimeras highlighted that this reduction in MPP numbers involved a cell-autonomous defect (Fig. 3 C). As the numbers of CMPs, GMPs and MEPs were normal in the BM of mutant mice, these data suggested that the pool of *Cxcr4*^{1013}-bearing MPPs is myeloid-biased, being profoundly depleted in lymphoid potential but still containing myeloid potential. Supporting this assumption, we observed increased frequency of myeloid-biased CD150^{high} LSK CD34$^-$ cells in the BM of 1013/1013 mice (Fig. 3 D; Young et al., 2016).

LSK CD48$^-$CD150$^+$ (signaling lymphocyte activation molecule [SLAM]) HSCs that encompass LSK Flt3$^-$ CD34$^-$CD48$^-$CD150$^+$ (long-term [LT]) and LSK Flt3$^-$CD34$^+$ CD48$^-$CD150$^+$ (short-term [ST]) subsets precede MPPs in the hematopoietic differentiation tree (Fig. S1 A). We hypothesized that the overall myeloid skewing of mutant HSCs contributes to the reduction in lymphoid potential of MPPs and, consequently, in committed downstream lymphoid progenitors. To test this, we first quantified the number of MPPs that could be generated in vitro from WT and mutant LSK SLAMs. Similar numbers of sorted LSK SLAMs from the BM of WT and mutant mice were cultured for up to 4 d in feeder-free media in the presence of a set of cytokines (Cho et al., 1999; Nie et al., 2008; Tsai et al., 2013). Both frequencies and numbers of MPPs were slightly but significantly lower in *Cxcr4*^{1013}-bearing cell cultures compared with the WT ones over the course of the assay (Fig. 3 E). Second, we sought to determine whether *Cxcr4*^{1013}-carrying MPPs contained cells capable to differentiate into LMPPs. We found that *Cxcr4*^{1013}-bearing MPPs were less efficient at producing LMPPs by days 2 and 4 compared with WT cells (Fig. 3 G). The proliferation status did not differ between WT and mutant HSPCs (Fig. 3, F and H).

Finally, we examined in vitro the function of the Cxcl12/Cxcr4 axis in HSPCs. Membrane expression of Cxcr4 was similar between WT and mutant BM HSPCs (Fig. 3 I). However, +/1013 and 1013/1013 Lin$^-$ cells, which include HPSCs, displayed both impaired Cxcr4 internalization after Cxcl12 stimulation and increased Cxcl12-promoted chemotaxis (Fig. 3, J and K). Thus, the desensitization-resistant C-tail–truncated Cxcr4^{1013} receptor is functionally expressed on HSPCs and leads to hypersensitivity to Cxcl12. Abnormal Cxcr4 signaling was not associated with changes in apoptosis of lymphoid progenitors (Fig. 3 L). These findings indicate that Cxcr4 desensitization regulates differentiation of HSCs into MPPs and further report a previously unanticipated role for such regulatory process in the MPP-to-LMPP transition.

mice. Data are from three independent experiments with five to seven mice per group. (G) Schematic diagram for the generation of long-term BM chimeras. (H) Absolute numbers of donor CD45.2$^+$ (WT, +/1013, or 1013/1013) total CD3$^+$ T and B220$^+$ B cells, pro–B cells, and ETPs recovered from the blood, BM, and thymus of BM chimeras in CD45.1$^+$ (WT) recipients. Data are from at least three independent experiments with 6–12 recipient mice per group. (I) Absolute numbers of donor CD45.2$^+$ myeloid cells recovered from the blood and BM of BM chimeras in CD45.1$^+$ recipients. Data are from at least three independent experiments with 6–12 recipient mice per group. All displayed results are represented as means ± SEM. Kruskal–Wallis *H* test–associated p-values (#) are indicated. *, P < 0.05; **, P < 0.005; and ***, P < 0.0005 compared with WT or CD45.2$^+$ donor WT cells; §, P < 0.05; and §§, P < 0.005 compared with +/1013 or CD45.2$^+$ donor +/1013 cells (as determined using the two-tailed Student's *t* test).

Increased quiescence of *Cxcr4*^{1013}-bearing ST-HSCs in the BM

We next investigated the impact of the *Cxcr4* mutation on BM HSC homeostasis. Compared with WT mice, mutant mice had normal numbers of LSK and LSK SLAMs, including both LT- and ST-HSC subpopulations (Fig. 4 A and Fig. S1 [A and C] for flow cytometry analyses). Relevant functions of Cxcl12/Cxcr4 signaling in HSC biology include regulating their quiescence (Nie et al., 2008; Tzeng et al., 2011). We observed a slight but significant increase in proportions of BM LSK SLAM cells in the quiescent G0 state (DAPI^{low}Ki-67^{-}) in mutant mice (Fig. 4 B). The latter was particularly evident in 1013/1013 ST-HSCs and spared the LT-HSC pool. We also examined the effect of intraperitoneal injection of 5-fluorouracil (5-FU), which selectively eliminates cycling but not quiescent HSCs. After a single dose of 5-FU, we observed higher numbers of ST-HSCs in mutant mice that follow an allele dose-dependent fashion compared with WT controls (Fig. 4 C). We next evaluated how fast mutant ST-HSCs would divide by performing BrdU label–retaining cell (LRC) assays. Consistent with the DAPI/Ki-67 staining, we observed after a 12-d pulse period a *Cxcr4*^{1013} allele dose-dependent reduction in BrdU incorporation within mutant ST-HSCs compared with WT ones (Fig. 4 D). After 3 wk of chase, ST-HSCs carrying or not the *Cxcr4* mutation had lost most of LRC activity. We also examined the expression levels of selected regulators of the cell cycle machinery by quantitative real-time PCR in ST-HSCs sorted from the BM of WT and mutant mice. We focused on expression of genes encoding D-type cyclins (D1–D3), which regulate G1-S transition notably in HSPCs and inversely correlate with CXCR4 expression (Nie et al., 2008; Tsai et al., 2013). Consistent with the increased quiescent status of mutant ST-HSCs, levels of *D-cyclin* mRNAs were significantly decreased in 1013/1013 ST-HSCs over control cells (Fig. 4 E). This was corroborated at the protein level as shown by flow cytometry stains for cyclin D3 (Fig. 4 F). Together, these findings reveal that the quiescence/cycling balance is disturbed in *Cxcr4*^{1013}-bearing BM ST-HSCs.

Impaired homing, multipotency, and self-renewal properties of *Cxcr4*^{1013}-bearing HSCs

Aforementioned findings suggest that *Cxcr4*^{1013}-bearing HSPCs exhibit impaired lymphoid capacity associated with a myeloid-bias, which together evoke an aging-induced shift in HSC composition (Young et al., 2016). In line with this, middle-aged (56 wk old) WT mice displayed increased number of LT-HSCs (Figs. 4 A and 5 A). Numbers of LSK SLAMs were higher in the BM of mutant mice than in that of WT mice, proportional to *Cxcr4*^{1013} allele dose. This was observed in both LT- and ST-HSC populations (Fig. 5 A). The proportions of LT- and ST-HSCs in the quiescent G0 state were slightly but significantly decreased in the BM of middle-aged mutant mice (Fig. 5 B). These results indicate that the desensitization-resistant Cxcr4^{1013} receptor is associated with changes in the quiescence/cycling balance in *Cxcr4*^{1013}-bearing BM HSCs and their expansion with age. Serial BM transplantation is considered in many aspects as a stress setting (Karpova and Bonig, 2015), in which both the multipotency and self-renewal abilities of HSCs can be assessed in vivo. Primary engraftments were accomplished by transferring BM cells from young (8–12 wk old) CD45.2^{+} WT or mutant mice into lethally irradiated young CD45.1^{+} WT recipients. Four months later, BMs from these chimeric mice were transferred into a second set of lethally irradiated young CD45.1^{+} WT recipients. After primary reconstitution, there was a marked reduction in frequency and absolute number of CD45.2^{+} LSK SLAM in the BM of CD45.1^{+} WT recipients engrafted with 1013/1013 BM, but no defect in BM reconstitution using +/1013 HSCs (Fig. 5 C). In secondary transplantation, a dramatically reduced contribution of *Cxcr4*^{1013}-bearing CD45.2^{+} HSCs to the BM of WT recipients highlighted the decreased capacity for self-renewal of these cells (Fig. 5 D). In reverse chimeras, the proportion and number of BM CD45.1^{+} LSK and LSK SLAM cells were comparable between experimental groups (Fig. 2 D), indicating that impaired reconstitution capacity of mutant HSCs occurs in a cell-intrinsic manner. In vivo homing assays revealed a *Cxcr4*^{1013} allele dose-dependent reduction in the BM homing potential of LSK and LSK SLAM (Fig. 5, E and

Table 1. **Blood characterization in WT and *Cxcr4*^{1013}-bearing mice**

Blood parameters	WT (*n* = 12)	+/1013 (*n* = 10)	1013/1013 (*n* = 11)
White blood cells (10^3/mm^3)[a]	5.0 ± 1.5	1.6 ± 0.2[b]	1.0 ± 0.3[b,c]
Red blood cells (10^6/mm^3)	9.3 ± 0.7	9.4 ± 0.4	9.1 ± 0.7
Mean corpuscular volume (Fl)	50.2 ± 0.9	49.5 ± 0.6	49.0 ± 1.4
Platelets (10^3/mm^3)	931.7 ± 113.2	915.4 ± 58.2	924.1 ± 67.2
Hematocrit (%)	47.0 ± 2.9	46.7 ± 2.0	46.1 ± 3.1
Hemoglobin (g/dl)	15.7 ± 0.9	16.0 ± 1.1	15.0 ± 1.4

Data are means ± SEM.

[a]$P < 0.0005$ for this parameter, determined using the Kruskal–Wallis *H* test.

[b]$P < 0.0005$ compared with WT mice, determined using the unpaired two-tailed Student's *t* test.

[c]$P < 0.005$ compared with +/1013 mice, determined using the unpaired two-tailed Student's *t* test.

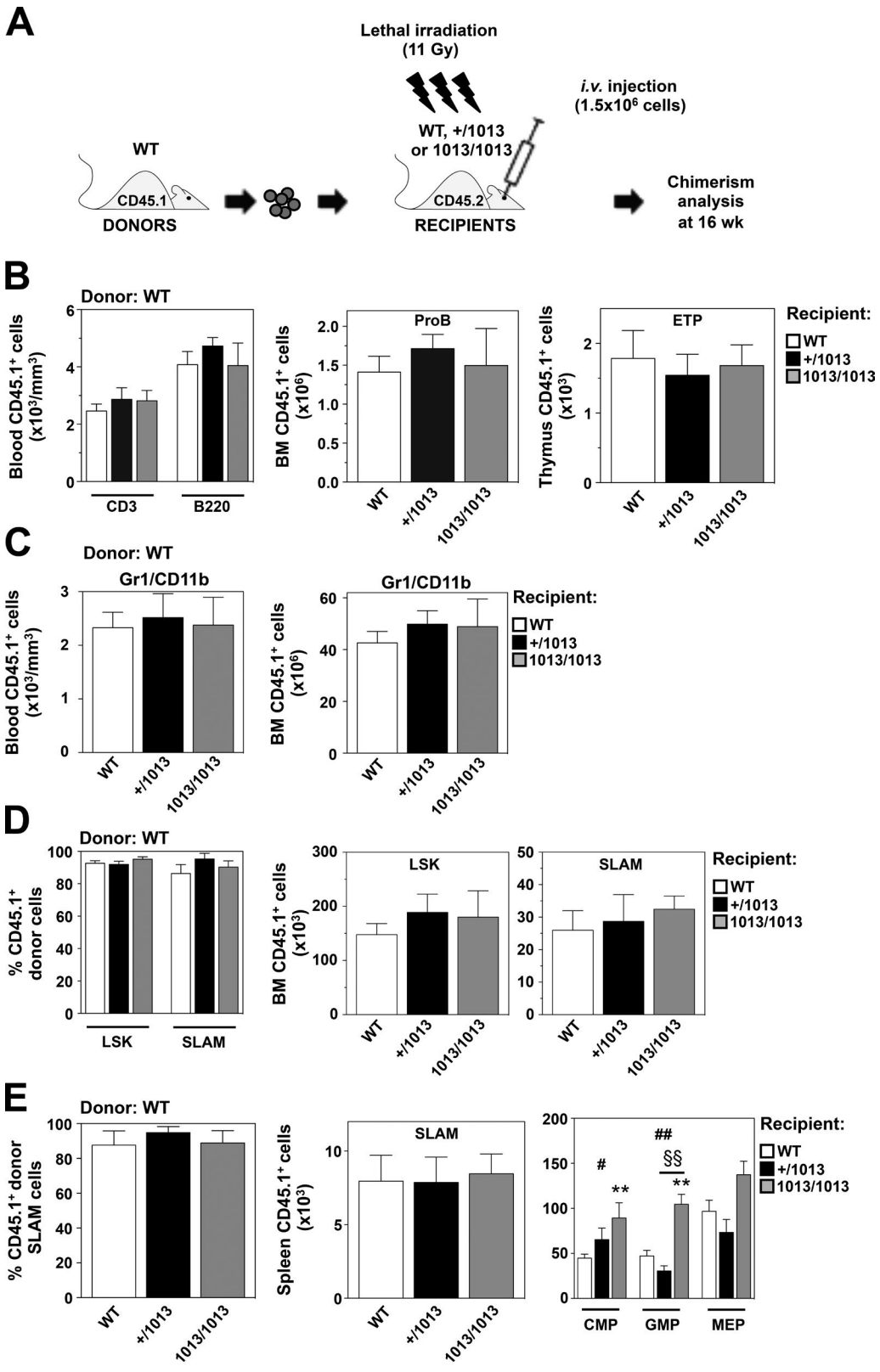

Figure 2. **Impact of *Cxcr4*^{1013}-bearing nonhematopoietic cells on hematopoiesis.** (A) Schematic diagram for the generation of long-term BM chimeras. (B) Absolute numbers of donor CD45.1$^+$ (WT) total CD3$^+$ T and B220$^+$ B cells, pro–B cells, and ETPs recovered from the blood, BM, and thymus of BM chimeras in CD45.2$^+$ (WT, +/1013 or 1013/1013) recipients. Data are from at least three independent experiments with 6–10 recipient mice per group.

F). Collectively these findings show that the in vivo homing potential of *Cxcr4*^{1013}-bearing HSCs is impaired, indicating that efficient Cxcr4 desensitization is required for BM engraftment and reconstitution.

Abnormal distribution of *Cxcr4*^{1013}-bearing HSPCs in the periphery

The Cxcl12/Cxcr4 pair regulates HSPC retention in and egress from the BM (Broxmeyer et al., 2005; Foudi et al., 2006; Nie et al., 2008; Christopher et al., 2009). We explored whether the *Cxcr4* mutation affected the peripheral distribution of HSPCs. We found that the number of CFU-Cs in blood of mutant mice was decreased in a *Cxcr4*^{1013} allele dose-dependent fashion (Fig. 6 A). A similar phenomenon was observed in blood samples drawn from two unrelated and two related patients with WS and carrying distinct autosomal-dominant mutations in *CXCR4*. There were significant reductions in the number of CFU-Cs, HSCs/MPPs (defined as CD45RA$^-$CD38$^-$CD34$^+$), and immature multilymphoid progenitors (MLPs; defined as CD45RA$^+$CD38$^-$CD7$^-$CD34$^+$CD10$^+$) in the circulation of patients compared with healthy individuals (Fig. 6, B and C; and Fig. S1 D). This pattern of HSPC dysfunctions was extended to the blood of a WHIM^{WT} patient that was reported to display impaired CXCR4 desensitization to CXCL12 (Balabanian et al., 2005, 2008). These findings suggest an abnormal recirculation of mutant HSPCs in both mice and humans.

To determine the role of the *Cxcr4* mutation in a stressed mobilization situation, we assessed the impact of a single intraperitoneal injection of the Cxcr4 antagonist AMD3100 on HSPC distribution in the blood of WT and mutant mice. 1 h after injection, AMD3100-mediated inhibition of Cxcr4 signaling in WT mice led to a significant increase in the absolute numbers of circulating HSPCs (Fig. 6 D). Mutant HSPCs were also sensitive to hematopoietic insults, as AMD3100 treatment increased their absolute numbers in the blood, reaching that observed in untreated WT mice. Thus, enforced mobilization of HSPCs with AMD3100 was apparently normal in mice carrying desensitization-resistant Cxcr4 receptors.

We next sought to determine the representation of *Cxcr4*^{1013}-bearing HSPCs in the spleen, where hematopoiesis can expand under specific settings, a process referred to as extramedullary hematopoiesis (EMH; Wolf and Neiman, 1987; Morrison et al., 1997; Baldridge et al., 2010). We observed that mutant mice displayed significantly increased frequencies and numbers of splenic LSK SLAMs in a *Cxcr4*^{1013} allele dose-dependent fashion (Fig. 6 E). Moreover, 1013/1013 spleens also had significantly increased numbers of CFU-Cs, CMPs, and GMPs compared with WT, whereas MEPs remained unchanged (Fig. 6 F). The substantial increase in splenic HSCs and subsets of myeloid-committed progenitors observed in young adult mutant mice compared with WT was even more pronounced in middle-aged mice, affecting CFU-Cs, CMPs, GMPs, and MEPs (Fig. 6 G). In vivo homing assays revealed increased numbers of Lin$^-$ cells recovered from the spleens of WT CD45.1$^+$ recipients injected with mutant CD45.2$^+$ BM cells (Fig. 6 H). This suggests that enhancement of EMH might be a consequence of increased homing of *Cxcr4*^{1013}-bearing HSPCs from circulation to spleen. Similar to full mice (Fig. 6, E and F), the numbers of splenic LSK SLAM, CMPs, and GMPs were increased in *Cxcr4*^{1013}-carrying BM chimeras compared with WT chimeras (Fig. 6 I). In reverse chimeras, the numbers of splenic LSK SLAMs were comparable in all experimental groups, whereas myeloid progenitors were increased in the spleen of 1013/1013 recipients (Fig. 2 E). These results indicate that the expansion of LSK SLAMs is predominantly intrinsic to the gain of Cxcr4 function in HSCs, whereas that of the myeloid progenitors involves both intrinsic and extrinsic defects.

Splenic EMH is associated with increased detection of Cxcl12 in *Cxcr4*^{1013}-bearing mice

During splenic EMH, HSCs predominantly localize around sinusoids in the red pulp, where Cxcl12 is expressed by sinusoidal endothelial cells in humans and a subset of perivascular stromal cells in mice (Miwa et al., 2013; Inra et al., 2015). Notably, EMH induction in mice was found to expand stromal cells by promoting their proliferation (Inra et al., 2015). Thus, we examined the Cxcl12 status in the spleen of adult *Cxcr4*^{1013}-bearing mice, where enhanced EMH develops under steady-state conditions. By quantitative real-time PCR, we found that transcripts encoding Cxcl12 were detectable at similar level in the spleens of both WT and *Cxcr4*^{1013}-bearing mice (Fig. 7 A). However, the Cxcl12 protein was significantly increased in spleen supernatants from 1013/1013 mice (Fig. 7 B). This would be consistent with increased Cxcl12 production by an expanded but still numerically small population of stromal cells in adult spleen of *Cxcr4*^{1013}-bearing mice. Thus, we performed immunostainings on splenic sections from WT and mutant mice to better delineate the source of Cxcl12. Cxcl12 staining was significantly stronger in mutants than in WT spleens in a *Cxcr4*^{1013}

(C) Absolute numbers of donor CD45.1$^+$ (Gr1$^+$CD11b$^+$) myeloid cells recovered from the blood and BM of BM chimeras in CD45.2$^+$ recipients. Data are from at least two independent experiments with four to nine recipient mice per group. (D) Proportions (left) and absolute numbers (middle and right) of donor CD45.1$^+$ LSK and LSK SLAM recovered from the BM of chimeras in CD45.2$^+$ recipients. Data are from at least three independent experiments with 6–15 recipient mice per group. (E) Proportions (left) and absolute numbers (middle and right) of donor CD45.1$^+$ LSK SLAM, CMPs, GMPs, and MEPs recovered from the spleens of chimeras in CD45.2$^+$ recipients. Data are from at least three independent experiments with 6–15 recipient mice per group. All displayed results are represented as means ± SEM. Kruskal–Wallis *H* test–associated p-values (#) are indicated. **, $P < 0.005$; and §§, $P < 0.005$ compared with WT and +/1013 recipients, respectively (as determined using the two-tailed Student's *t* test).

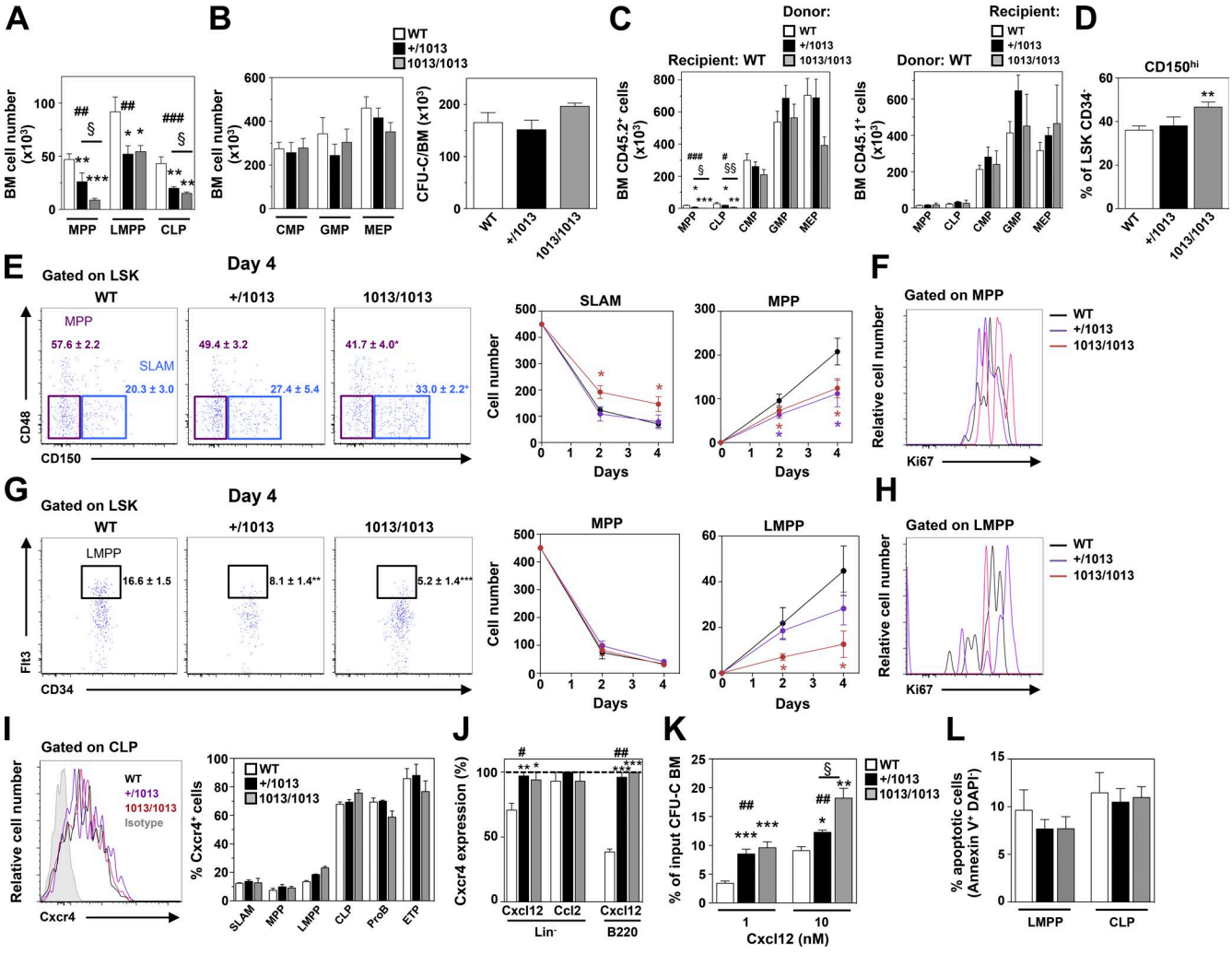

Figure 3. ***Cxcr4*^{1013}-bearing mice display a cell-intrinsic constraint in multipotent and lymphoid-biased progenitors in the BM.** (A) Absolute numbers of MPPs (Lin$^-$c-Kit$^+$Sca-1$^+$ [LSK] CD48$^-$CD150$^-$), LMPPs (LSK Flt3^{high}CD34$^+$), and CLPs (Lin$^-$c-Kit^{low}Sca-1^{low}Flt3$^+$CD127$^+$) in the BM of WT and mutant mice. Data are from at least four independent experiments with 13–17 mice per group. (B, left) Absolute numbers of CMPs (Lin$^-$c-Kit$^+$Sca-1$^-$CD34$^+$CD16/32$^-$), GMPs (Lin$^-$c-Kit$^+$Sca-1$^-$CD34$^+$CD16/32$^+$), and MEPs (Lin$^-$c-Kit$^+$Sca-1$^-$CD34$^-$CD16/32$^-$). (right) Number of colonies formed from WT, +/1013, or 1013/1013 BM in the myeloid lineage in CFU-C assays. Data are from at least four independent experiments with 7–10 mice per group. (C) Absolute numbers of donor CD45.2$^+$ (left, WT, +/1013, or 1013/1013) or CD45.1$^+$ (right, WT) MPPs, CLPs, CMPs, GMPs, and MEPs recovered from the BM of chimeras in CD45.1$^+$ (left, WT) or CD45.2$^+$ (right, WT, +/1013 or 1013/1013) recipients. Data are from at least three independent experiments with 8–15 recipient mice per group. (D) Frequency of CD150^{high} in LSK CD34$^-$ cells in the BM of young WT and mutant mice. Data are from at least four independent experiments with 6–10 mice per group. (E and G) Equal numbers of purified LSK SLAM (CD48$^-$CD150$^+$; E) or MPPs (G) were cultured for 4 d in a cytokine-supplemented feeder-free media. (left) Representative flow cytometric analyses comparing the frequencies of LSK SLAM and MPPs (E) or LMPPs (G) at day 4. (right) Absolute numbers of LSK SLAM and MPPs (E) and of MPPs and LMPPs (G) after 2 and 4 d of culture. Data are from three independent experiments with six mice per group. (F and H) Representative histograms for the expression of Ki-67 in MPPs (F) and LMPPs (H) after 4 d of culture. (I, left) Membrane expression of Cxcr4 was determined by flow cytometry on gated BM CLPs from WT, +/1013, and 1013/1013 mice. Background fluorescence is shown (isotype, gray histograms). (right) The percentages of LSK SLAM, MPPs, LMPPs, CLPs, pro–B cells, and ETPs expressing Cxcr4 are shown. Data are from three independent experiments with five to seven mice per group. (J) Cell surface expression of Cxcr4 on BM Lin$^-$ cells or B220$^+$ B cells upon exposure to 10 nM Cxcl12 or 100 nM Ccl2 at 37°C for 45 min. No Cxcr4 internalization was found when cells were incubated at 4°C in the presence of Cxcl12. Cxcr4 expression on BM cells incubated in medium alone was set at 100% (dotted horizontal line). Data are from three independent experiments with five mice per group. (K) Migration of Lin$^-$ BM cells from WT, +/1013, and 1013/1013 mice in response to 1 or 10 nM of Cxcl12 was enumerated by CFU-C assays. Data are from at least three independent experiments with five to eight mice per group. (L) The proportions of apoptotic (Annexin V$^+$ DAPI$^-$) LMPPs and CLPs were determined by flow cytometry in the BM of WT and mutant mice. Data are from three independent experiments with eight to nine mice per group. All displayed results are represented as means ± SEM. Kruskal–Wallis *H* test–associated p-values (#) are indicated. *, $P < 0.05$; **, $P < 0.005$; and ***, $P < 0.0005$ compared with WT or CD45.2$^+$ donor WT cells; §, $P < 0.05$; and §§, $P < 0.005$ compared with +/1013 or CD45.2$^+$ donor +/1013 cells (as determined using the two-tailed Student's *t* test).

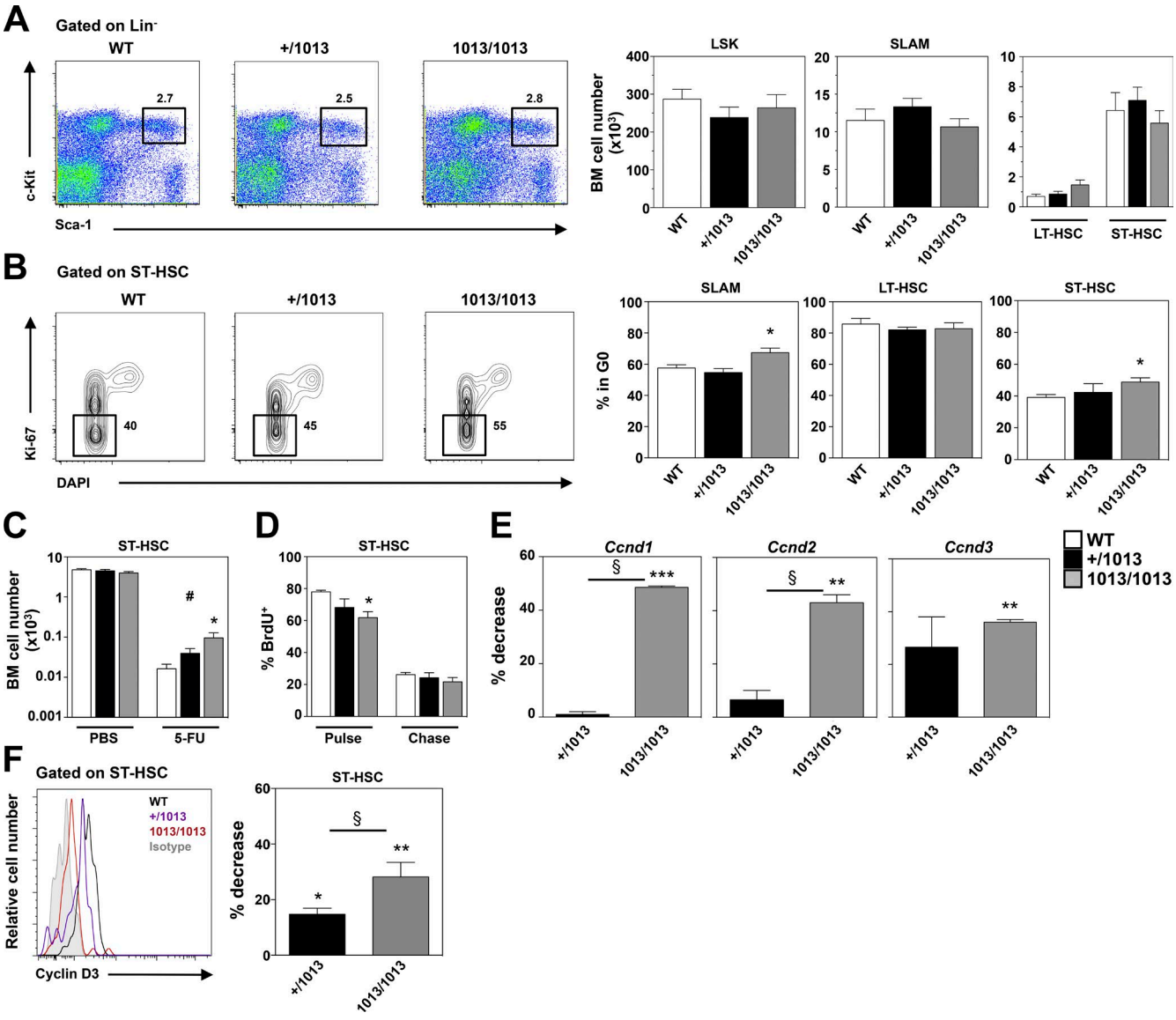

Figure 4. ***Cxcr4*^{1013}-bearing HSCs exhibit changes in the quiescence/cycling balance in the BM.** (A, left) Representative flow cytometric analyses comparing WT, +/1013, and 1013/1013 LSK frequencies in the BM. (right) Absolute numbers of LSK, LSK SLAM, LT-HSCs (LSK Flt3$^-$CD34$^-$CD48$^-$CD150$^+$), and ST-HSCs (LSK Flt3$^-$CD34$^+$CD48$^-$CD150$^+$). Data are from at least four independent experiments with 13–17 mice per group. (B) Ki-67 and DAPI costaining was used to analyze by flow cytometry the cell cycle status of LSK SLAM, LT-HSC, and ST-HSC subsets in the BM. (left) Representative flow cytometric analysis of ST-HSCs in the BM of WT, +/1013, and 1013/1013 mice. (right) Bar graphs showing the percentage of cells (DAPI^{low}Ki-67$^-$) in the quiescent G0 phase. Data are from at least three independent experiments with five to nine mice per group. (C) Absolute numbers of BM ST-HSCs 3.5 d after a single dose of PBS or 5-FU. Data are from three independent experiments with six mice per group. (D) Percentage of BrdU$^+$ in ST-HSCs after a 12-d pulse period (pulse) and after 3 wk of chase (chase). Data are from two independent experiments with four to eight mice per group at each time point. (E) Expression levels of D-cyclins (*Ccnd1*, *Ccnd2*, and *Ccnd3*) were determined by quantitative real-time PCR in ST-HSCs sorted from the BM of WT and mutant mice. Each individual sample was run in triplicate with eight mice per group and has been standardized for *β-actin* expression levels. Results are expressed as percentage of decrease in mutant ST-HSCs compared with the levels obtained in WT ones (set at 100%). (F, left) Representative histograms for intracellular detection of cyclin D3 by flow cytometry in gated BM ST-HSCs from WT and mutant mice. (right) Bar graphs denote the percentage of decrease in cyclin D3 MFI values in mutant ST-HSCs compared with the levels obtained in WT ones (set at 100%). Data are from two independent experiments with six mice per group. All displayed results are represented as means ± SEM. Kruskal–Wallis *H* test–associated p-values (#) are indicated. *, $P < 0.05$; **, $P < 0.005$; and ***, $P < 0.0005$ compared with WT cells; §, $P < 0.05$ compared with +/1013 cells (as determined using the two-tailed Student's *t* test).

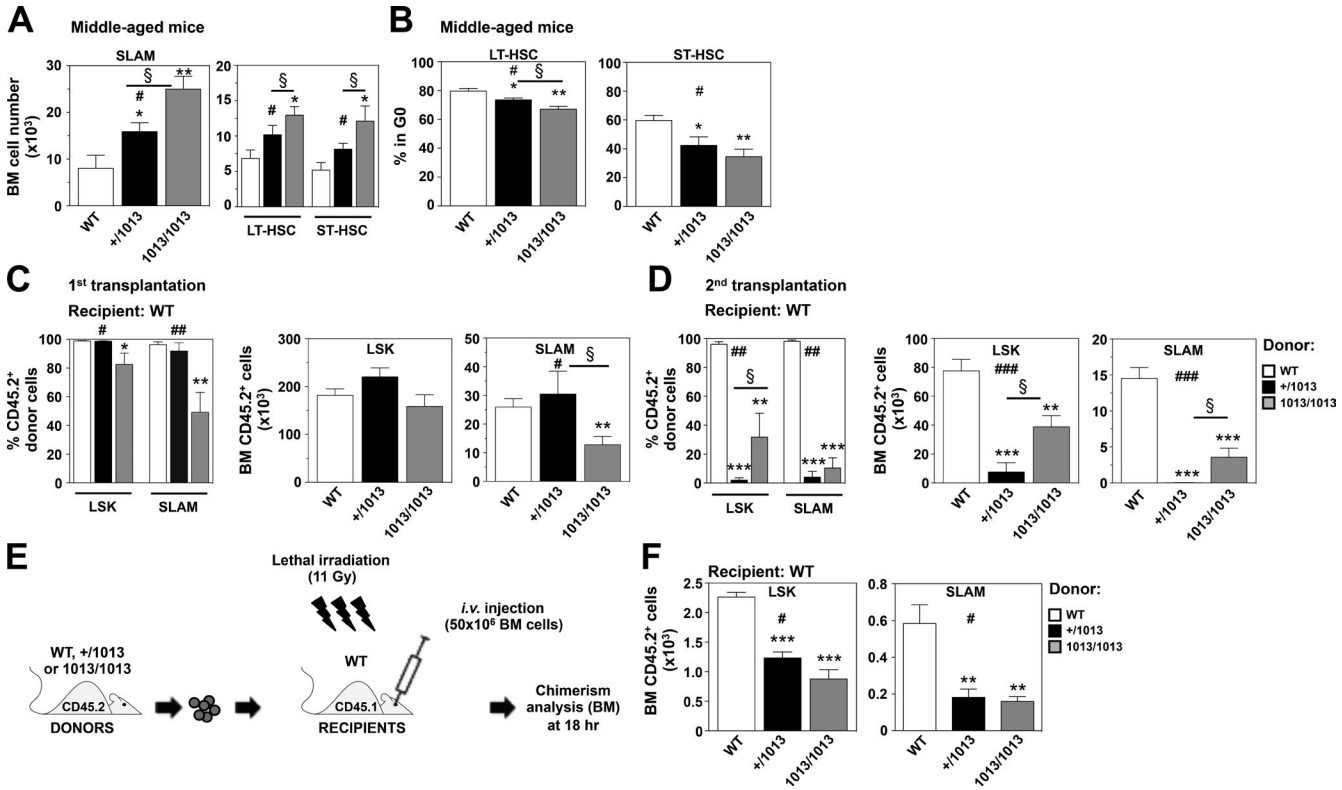

Figure 5. ***Cxcr4*^{1013}–bearing HSCs display disturbed homing, multipotency, and self-renewal capacities.** (A) Absolute numbers of LSK SLAM, LT-HSCs, and ST-HSCs in the BM of middle-aged (56 wk old) WT, +/1013, and 1013/1013 mice. Data are from at least four independent experiments with 6–10 mice per group. (B) Bar graphs showing the percentage of LT-HSCs and ST-HSCs in the quiescent G0 phase (DAPI^{low}Ki-67^{-}) in the BM of middle-aged mice. Data are from two independent experiments with five mice per group. (C) Proportions (left) and absolute numbers (middle and right) of CD45.2^{+} LSK and LSK SLAM from WT, +/1013, or 1013/1013 young (8–12 wk old) donor mice, recovered from the BM of chimeras in young CD45.1^{+} (WT) recipients after primary transplantation. Data are from at least three independent experiments with 8–15 recipient mice per group. (D) Serial transplantation of total donor CD45.2^{+} (WT, +/1013, or 1013/1013) cells recovered from the BM of primary BM chimeras in young CD45.1^{+} (WT) recipients. Proportions (left) and absolute numbers (middle and right) of donor CD45.2^{+} LSK and LSK SLAM were assessed in the BM of lethally irradiated CD45.1^{+} (WT) recipients 4 mo after secondary BM transplants. Data are from three independent experiments with 6–10 recipient mice per group. (E) Schematic diagram for in vivo homing assays of CD45.2^{+} (WT, +/1013, or 1013/1013) BM cells into lethally irradiated CD45.1^{+} WT recipients. (F) Absolute numbers of CD45.2^{+} LSK and LSK SLAM were determined by flow cytometry in the BM of recipients 18 h after injection. Data are from two experiments with four to five recipients per group. All displayed results are represented as means ± SEM. Kruskal–Wallis *H* test–associated p-values (#) are indicated. *, P < 0.05; **, P < 0.005; and ***, P < 0.0005 compared with WT or CD45.2^{+} donor WT cells; §, P < 0.05 compared with +/1013 or CD45.2^{+} donor +/1013 cells (as determined using the two-tailed Student's *t* test).

allele dose-dependent manner (Fig. 7 C). Consistent with previous studies (Miwa et al., 2013; Inra et al., 2015; Wang et al., 2015), Cxcl12 was primarily detected in the red pulp, although some white pulp central arterioles also stained positive. Tcf21-positive perivascular stromal cells were markedly expanded in the spleens of mutant mice and further identified as a source of Cxcl12 in the red pulp (Fig. 7, D and E). Thus, increased Cxcl12 in the spleen of *Cxcr4*^{1013}-bearing mice was observed in the setting of an abnormal expansion of Tcf21^{+} stromal cells during EMH.

DISCUSSION

In this study, we investigated the role of Cxcr4 desensitization in hematopoiesis using a unique knock-in mouse model expressing the naturally occurring WS-linked heterozygous gain-of-function *Cxcr4* mutation. We demonstrated for the first time an allele dose effect of the *Cxcr4*^{1013} mutation on the severity of the lymphohematopoietic phenotype. We also provided evidence that Cxcr4 desensitization regulates at multiple stages several aspects of HSPC homeostasis by altering the balance between quiescence and differentiation of HSPC subsets. When Cxcr4 desensitization is impaired, it results in defective generation of lymphoid-committed progenitors in BM and promotes abnormal HSPC expansion and enhanced myeloid-biased EMH in the spleen. Moreover, HSPCs were barely detectable in the peripheral blood of *Cxcr4*^{1013}-bearing mice, and importantly, of five patients with WS. Thus, we propose that *Cxcr4*^{1013}-driven deregulation of the lymphohematopoiesis process accounts for the lymphopenia observed in mice and likely in WS patients.

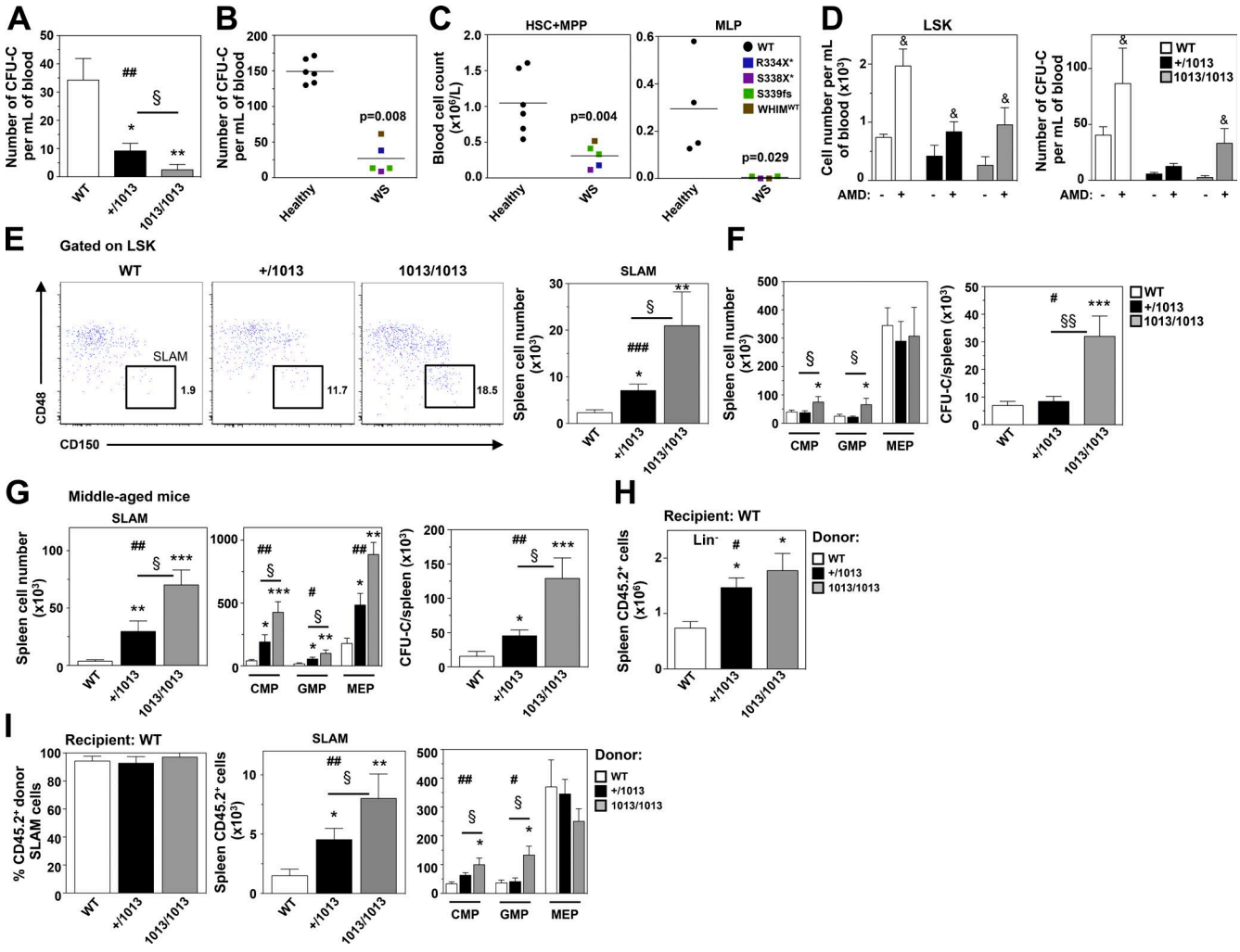

Figure 6. ***Cxcr4*^{1013}-bearing HSPCs abnormally compartmentalize in the periphery.** (A) Number of CFU-Cs in peripheral blood of WT, +/1013, and 1013/1013 mice. Data are from at least four independent experiments with 7–15 mice per group. (B) Number of CFU-Cs in the bloodstream of healthy individuals and WS patients carrying (R334X*, S338X*, and S339fs) or not (WHIM^{wt}) a disease *CXCR4* allele. Lines indicate the mean and each symbol represent one subject. (C) Relative numbers of HSCs plus MPPs ($Lin^-CD45RA^-CD38^-CD34^+$, left) and immature lymphoid progenitors (MLP, $Lin^-CD45RA^+CD38^-CD7^-CD34^+CD10^+$, right) were determined by flow cytometry in the blood of healthy and WS subjects. (D) Numbers of LSK (left) or CFU-Cs (right) were determined in the blood of WT and mutant mice 1 h after intraperitoneal injection of AMD3100 (+) or PBS (–). Data are from two independent experiments with five mice per group. (E, left) Representative flow cytometric analyses comparing WT, +/1013, and 1013/1013 LSK SLAM frequencies in the spleen. (right) Absolute numbers of splenic LSK SLAM. Data are from at least five independent experiments with 9–15 mice per group. (F, left) Absolute numbers of CMPs, GMPs, and MEPs in the spleen. (right) Numbers of colonies formed from WT, +/1013, and 1013/1013 spleens in the myeloid lineage in CFU-C assays. Data are from at least four independent experiments with 7–15 mice per group. (G) Numbers of LSK SLAM, CMPs, GMPs, MEPs, and CFU-Cs in the spleen of middle-aged (56 wk old) WT, +/1013, and 1013/1013 mice. Data are from at least four independent experiments with 6–10 mice per group. (H) In vivo homing assays of $CD45.2^+$ (WT, +/1013, or 1013/1013) BM cells into lethally irradiated $CD45.1^+$ WT recipients. Absolute numbers of $CD45.2^+$ Lin^- cells were determined by flow cytometry in the spleen of recipients 18 h after injection. Data are from two experiments with four to five recipients per group. (I) Proportions (left) and absolute numbers (middle and right) of donor $CD45.2^+$ (WT, +/1013, or 1013/1013) LSK SLAM, CMPs, GMPs, and MEPs recovered from the spleen of BM chimeras in $CD45.1^+$ (WT) recipients. Data are from at least three independent experiments with 6–12 recipient mice per group. All displayed results are represented as means ± SEM. Kruskal–Wallis *H* test–associated p-values (#) are indicated. Two-tailed Student's *t* tests (A and D–I) or the Mann–Whitney *U* test (B and C) were used to assess statistical significance (*, $P < 0.05$; **, $P < 0.005$; and ***, $P < 0.0005$ compared with WT or $CD45.2^+$ donor WT cells; §, $P < 0.05$; and §§, $P < 0.005$ compared with +/1013 or $CD45.2^+$ donor +/1013 cells; &, $P < 0.05$ compared with PBS-treated mice).

Mice with a gain-of-*Cxcr4*-function mutation leading to a truncated C-tail of the resulting membrane protein have a higher proportion of quiescent G0 cells, in particular among the ST-HSC subset. This was associated with decreased expression of *D-Cyclin* products, thus reinforcing the importance of Cxcr4 desensitization in controlling HSPC proliferation and quiescence as suggested in mice deficient for *Cxcr4* (Sugiyama et al., 2006; Nie et al., 2008). HSCs from mutant

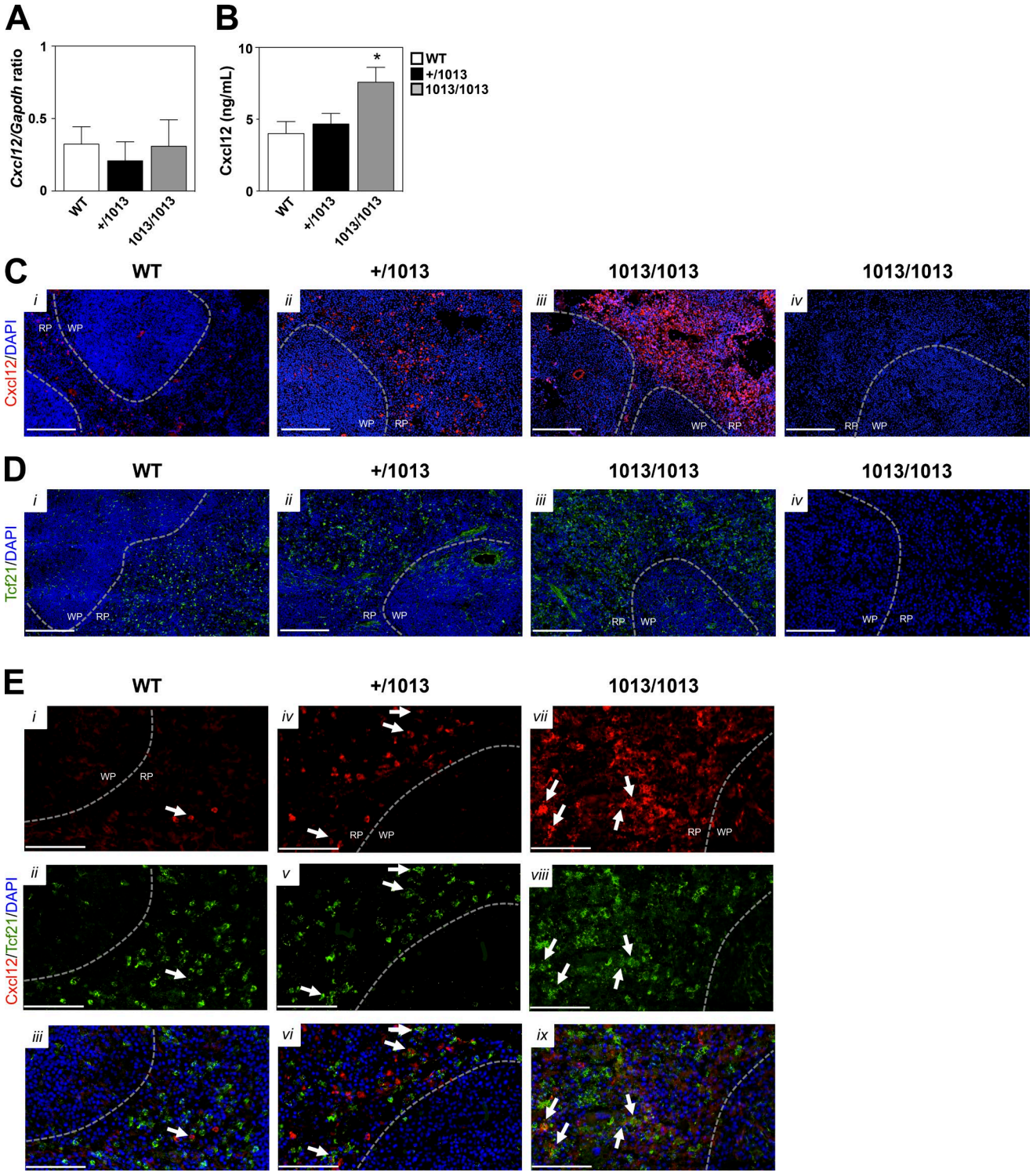

Figure 7. **Splenic Cxcl12 up-regulation in *Cxcr4*^{1013}-bearing mice.** (A) Levels of *Cxcl12* mRNAs in total spleen cells from WT, +/1013, and 1013/1013 mice were assessed by real-time quantitative PCR analyses. Each individual sample was run in triplicate with five mice per group, and results (mean ± SEM) are expressed as *Cxcl12*/*Gapdh* ratio. (B) Levels (mean ± SEM) of Cxcl12 were determined by ELISA in spleen supernatants from WT, +/1013, and 1013/1013 mice (n = 5 per group). (C–E) Spleen sections from WT, +/1013, and 1013/1013 mice were immunostained for Cxcl12 (C), Tcf21 (D), or both markers (E) in association with DAPI. The color code for antibodies used is shown. Negative controls (*iv*, C and D) to support the validity of staining were done by adding

mice, although displaying in vitro increased signaling through Cxcr4 upon Cxcl12 exposure, exhibited in vivo reduced homing to the BM associated with strong defects in hematopoietic reconstitution when serially injected into irradiated WT mice. In light of previous studies (Kawai et al., 2007; Lai et al., 2014; McDermott et al., 2015), these defects further establish the C-tail domain of Cxcr4 as an important regulator of the receptor function in HSC transplantation. With age, mutant mice displayed a significant expansion of the HSC pool and changes in their quiescence/cycling balance. Both diminished HSC serial transplant capacity and aging phenotype have been causally associated with increased intracellular oxidation stress (Ito et al., 2006; Shao et al., 2011; Yahata et al., 2011). Moreover, Cxcr4 signaling regulates oxidative stress in HSCs (Zhang et al., 2016) and, in turn, is a direct target of the oxidative stress regulator Nrf2 (Tsai et al., 2013). It would be important to determine whether Cxcr4 desensitization regulates reactive oxygen species levels in HSCs.

Our findings suggest that Cxcr4 desensitization is required for efficient ST-HSC-to-MPP transition and subsequently, for lymphoid specification and commitment in vivo. In the BM of mutant mice, we evidenced increased quiescence of ST-HSCs. This was associated with impaired multipotency of HSCs, suggesting that defective desensitization of Cxcr4 affects the differentiation of *Cxcr4*^{1013}-bearing ST-HSCs into MPPs by inducing a defect at the G0-G1 transition. In line with this, the length of the G1 phase has been reported to be crucial for the differentiation of neural stem cells as well as of HSCs (Kozar et al., 2004; Orford and Scadden, 2008). Absence of Cxcr4 desensitization also resulted in reduction in the numbers of LMPPs, CLPs, and ETPs in vivo, indicating a requirement for fine-tuned Cxcr4 signaling in lymphoid specification of HSPCs and/or maintenance of lymphoid-committed progenitors. Similarly, our in vitro differentiation assays unveiled an altered capacity of *Cxcr4*^{1013}-bearing LSK SLAMs to give rise to MPPs and that of MPPs to differentiate into LMPPs. Given that this was observed in a feeder-free media in the presence of necessary cytokines but without Cxcl12 addition, it is possible that progenitors that generate MPPs and LMPPs were already decreased from the LSK SLAM and MPP populations, respectively. As *Cxcr4*^{1013}-carrying HSCs exhibited a preserved ability to produce the earliest myeloid progenitors, one can speculate that only ST-HSCs that do not express myeloid genes exhibited increased quiescent status and failed to generate progenitors with lymphoid potential. Indeed, single-cell gene analyses pointed to the initiation of lymphoid-myeloid co-priming in a fraction of ST-HSCs and MPPs in vivo (Gautreau et al., 2010). Interestingly, conditional deletion of *Cxcr4* in MPPs reduced their differentiation into CLPs and decreased lymphopoiesis, suggesting that HSC niches instruct cell lineage decisions (Cordeiro Gomes et al., 2016). Thus, it is possible that enhanced Cxcr4 signaling results in abnormal positioning of HSPCs with a suboptimal access to critical factors controlling lineage decisions.

Concomitantly, *Cxcr4*^{1013}-carrying HSPCs abnormally compartmentalized in the periphery with a decrease in the blood mirrored by an accumulation in the spleen. Consistent with the work of Inra et al. (2015), we show that splenic EMH was associated with increased detection of Cxcl12 and expansion of Tcf21$^+$ stromal cells in the red pulp area. Cxcl12 was found to originate notably from Tcf21$^+$ stromal cells, thus suggesting a positive correlation between the number of HSCs and that of Tcf21$^+$ and Cxcl12$^+$ stromal cells. Cxcl12 increase in spleen may also result from its defective internalization by *Cxcr4*^{1013}-carrying stromal cells and/or HSPCs. Because Tcf21$^+$ stromal cells are reported as one of the component of the splenic perisinusoidal EMH niche (Inra et al., 2015) and circulating *Cxcr4*^{1013}-bearing Lin$^-$ cells display enhanced homing to the spleen, one would expect that Cxcl12 up-regulation contributes to enhancement of EMH in mutant mice.

Determining whether the lymphopenia exhibited by WS patients results from defective BM or thymus production or output of lymphocytes, exacerbated peripheral trapping and consumption of lymphocytes, or any combination of these has been an open question for several years. Pointing to defective hematopoiesis as causative is that umbilical cord blood stem cell transplantation has been reported to lead to a good outcome in a child with WS (Kriván et al., 2010). Additionally, a recent work has unveiled that a HSCs from a WS patient underwent chromothripsis, a complex chromosomal catastrophe that deleted notably the WS-linked allele *CXCR4*^{R334X}, allowing it to selectively repopulate the myeloid, but intriguingly not the lymphoid lineage (McDermott et al., 2015). This hematologic mosaicism suggests that the chromothriptic changes prevented differentiation of HSCs to CLPs, but not to CMPs, and the related underlying mechanisms. This hypothesis is supported by our findings in WS mice and extended observations made in patients. Analyses of blood samples from five patients carrying or not heterozygous *CXCR4* mutations but sharing a gain of CXCR4 function showed a severe reduction in circulating HSPCs, including MPPs and downstream lymphoid- and myeloid-committed progenitors. These findings pave the way for exploring in depth the BM of WS patients in search for a potential defect in HSPC generation and differentiation and shed new lights on how Cxcr4 desensitization regulates blood cell development and distribution.

the secondary antibody alone on 1013/1013 spleen sections. Dashed lines denote the boundary between the white pulp (WP) and red pulp (RP) areas. Arrows indicate the cells that colocalized Tcf21 and Cxcl12. Bars: (C and D) 200 µm; (E) 50 µm. Images are representative of four independent determinations. *, $P < 0.05$ compared with WT mice (as determined using the two-tailed Student's *t* test).

MATERIALS AND METHODS

Patients and HSPC analyses

All WS patients included in this study were registered in the French Severe Chronic Neutropenia Registry coordinated by J. Donadieu (Service d'Hématologie et Oncologie Pédiatrique, Trousseau Hospital, Paris). This registry has been labelized by the Comité National des Registres and has been allowed to collect data by the CCTIRS (#97-095) and the CNIL (#901062). Investigations of blood samples were performed in compliance with Good Clinical Practices and the Declaration of Helsinki. All individuals or parents for children have provided written informed consent before sampling, data registering, and genetic analyses. Patients P1 (9 yr old), P2, and P3 from the same family (41 and 9 yr old, respectively), P4 (11 yr old), and P5 (29 yr old) displayed clinical features of WS, including a marked leukopenia. At the time of the study, P1, P2, P3, P4, and P5 had a leukocyte count of 0.76×10^9/L, 1.07×10^9/L, 0.93×10^9/L, 0.85×10^9/L, and 2.6×10^9/L, respectively. Four of them had autosomal-dominant mutations in *CXCR4* (P1: c.1000C>T, p.Arg334*; P2 and P3: c.1013dup, p.Ser339Ilefs*5; and P4: c.1013C>G, p.Ser338*). P1 and P2 have been described previously (Beaussant Cohen et al., 2012), whereas P5 had a WT *CXCR4* coding sequence ($WHIM^{WT}$; Balabanian et al., 2005). Age- and sex-matched healthy blood donor volunteers were run in parallel and used as control subjects. Whole-blood phenotyping of HSPCs was performed as follows. In brief, 600 µl blood was labeled for 30 min at 4°C with a combination of the following conjugated mAbs: anti–human CD7 (clone M-T701, mouse IgG1), CD10 (clone HI10A, mouse IgG1), CD34 (clone 581, mouse IgG1), CD38 (clone HIT2, mouse IgG1), and CD45RA (clone HI100, mouse IgG2b). Antibodies were conjugated to brilliant violet (BV) 421, BV 605, FITC, APC, and AF700, and were purchased from BD. Corresponding isotype- and species-matched antibodies were used as negative controls. Thereafter, red blood cells were lysed with OptiLyse C buffer (Beckman Coulter) for 15 min at room temperature in the dark. Cells were analyzed on an LSR II Fortessa flow cytometer (BD). For functional analyses, 300 µl of blood cells was plated, after erythrocyte lysis with ACK (ammonium-chloride-potassium) buffer, in 35-mm tissue culture dishes into growth factor–supplemented methylcellulose medium (STEMCELL Technologies). After 2 wk of incubation at 37°C in 5% CO_2, CFU-Cs were enumerated under an inverted microscope.

Mice and genotyping

Cxcr4$^{+/1013}$ (+/1013) mice were generated by a knock-in strategy and bred as described previously (Balabanian et al., 2012). *Cxcr4*$^{1013/1013}$ (1013/1013) mice were obtained by crossing heterozygous +/1013 mice. WT mice were used as a control. All mice were littermates and age matched (8–12 or 56 wk old, referred as young or middle-aged, respectively). Adult Boy/J (CD45.1), WT, +/1013, and 1013/1013 (C57BL/6J background, CD45.2) mice were bred in our animal facility under 12 h light/dark cycle, specific pathogen-free conditions and feed ad libitum. All experiments were performed in accordance with the European Union guide for the care and use of laboratory animals and has been reviewed and approved by an appropriate institutional review committee (C2EA-26, Animal Care and Use Committee, Villejuif, France).

Sample isolation

BM cells were extracted by centrifugation from intact femurs and tibia, whereas spleens and thymus were gently mashed on a 70-µm nylon strainer to generate a single cell suspension. Cell collection was performed in PBS FCS 2% and filtered through a 70-µm nylon strainer. All cell numbers were standardized as total count per two legs, spleen, or thymus unless specified. Peripheral blood was collected by cardiac puncture. Red blood cell lysis was performed using ACK buffer before staining. Cells harvested from tissues were immunophenotyped immediately, incubated at 37°C for 60 min in RPMI 20 mM Hepes BSA 0.5% (Euromedex) before chemokine receptor internalization studies, or kept at 4°C overnight in PBS FCS 30% for chemotaxis assays.

Transplantation experiments and in vivo functional assays

For BM transplantation experiments, 1.5×10^6 total BM cells from young CD45.2$^+$ WT, +/1013, or 1013/1013 mice were injected into lethally irradiated young CD45.1$^+$ WT recipient mice (two rounds of 5.5 Gy separated by 3 h). Chimerism was analyzed 16 wk after reconstitution. Total BM from these mice was then transplanted into a second set of lethally irradiated young CD45.1$^+$ WT recipient mice (secondary transplantation). For reverse transplantation experiments, 1.5×10^6 total BM cells from CD45.1$^+$ WT mice were injected into lethally irradiated CD45.2$^+$ WT, +/1013, or 1013/1013 recipient mice. For in vivo homing assays, 50×10^6 cells from total BM of CD45.2$^+$ WT, +/1013, or 1013/1013 mice were injected into lethally irradiated CD45.1$^+$ WT recipient mice (two rounds of 5.5 Gy separated by 3 h). 18 h after injection, BM and spleen from recipient mice were harvested, and the homing pattern of CD45.2$^+$ Lin$^-$, LSK or LSK SLAM cells was evaluated by flow cytometry. 5-FU (InvivoGen) was injected intraperitoneally to mice at a dose of 150 mg/kg. PBS was used as control. Mice were sacrificed 3.5 d after injection, and the BM was analyzed by flow cytometry. Mice were treated with 5 mg/kg AMD3100 (Sigma-Aldrich) or PBS via intraperitoneal injection. 1 h later, peripheral blood was harvested, analyzed by flow cytometry, and tested for CFU-C assays.

In vitro functional assays

BM cells or splenocytes (10^5) and 100 µl blood cells after erythrocyte lysis were plated in duplicate in 35-mm tissue culture dishes in growth factor–supplemented methylcellulose medium. After 1 wk of incubation at 37°C in 5% CO_2, a mix of CFU-Cs was enumerated under an inverted microscope. For chemotaxis assays, 10^5 Lin$^-$ cells were added to the upper chambers of a 24-well plate with 5-µm-pore-size

Transwell inserts (EMD Millipore) containing or not different concentrations of Cxcl12 (R&D Systems) in lower chambers. Migrated cells were enumerated by CFU-C mix assay after 4 h of incubation at 37°C, 5% CO_2 and referred to input BM CFU-Cs to obtain a migration percentage. Cxcr4 internalization assay was performed as previously described (Balabanian et al., 2012) with some minor modifications. In brief, 10^7 BM cells were incubated at 37°C for 45 min with the indicated concentrations of Cxcl12 or Ccl2 (R&D Systems). The reaction was stopped by adding ice-cold RMPI and brief centrifugation at 4°C. After one wash in acidic glycine buffer, pH 4.3, levels of Cxcr4 membrane expression were determined by flow cytometry using the additional markers CD3, CD45R, Gr-1, CD11b, Ter119, and CD41 antigens. Background fluorescence was evaluated using the corresponding PE-conjugated immunoglobulin-isotype control antibody. Cxcr4 expression in stimulated cells was calculated as follows: (Cxcr4 geometric MFI of treated cells/Cxcr4 geometric MFI of unstimulated cells) × 100; 100% correspond to receptor expression at the surface of cells incubated in medium alone. For in vitro hematopoietic differentiation experiments, purified LSK SLAM or MPP cells were seeded at 450 cells into a 96-well tissue culture plate in DMEM medium supplemented with 10% FBS, 1% penicillin, and the following cytokines (5, 10, or 50 ng/ml): SCF, IL-3, IL-6, IL-7, and Flt3. Cells were cultured at 37°C in a humidified atmosphere containing 5% CO_2, and were harvested at the indicated intervals to analyze by flow cytometry differentiation and proliferation status (Ki-67 staining) of HSPCs.

Cell cycle and survival assays

For cell cycle analyses, purified BM Lin^- cells from WT and mutant mice were permeabilized and fixed according to the manufacturer's instructions with the FOXP3 permeabilization kit (Foxp3/Transcription Factor Staining Buffer Set) and then labeled with Ki-67 antibody (clone B56, mouse IgG1; BD) and DAPI before flow cytometric analysis. For label-retaining assays (Wilson et al., 2008), mice were injected intraperitoneally with 180 µg BrdU (Sigma-Aldrich) and maintained on water containing 800 µg/ml BrdU and 1% glucose during 12 d. The BrdU pulse was followed by a 3-wk chase period to detect by flow cytometry LRC activity by combining surface staining to define ST-HSCs with intracellular staining using the BrdU-FITC labeling kit following the manufacturer's instructions (BD). Cyclin D3 was detected by flow cytometry in fixed and permeabilized BM cells using a cyclin D3 mAb (clone 1/cyclin D3, mouse IgG2b; BD) followed by a secondary rat anti–mouse IgG2b PE-conjugated antibody (R&D Systems; Galloway et al., 2016). Apoptosis was measured using the active caspase-3–FITC apoptosis detection kit or the Annexin V apoptosis detection kit I (BD) followed by DAPI staining according to the manufacturer's instructions as described elsewhere (Balabanian et al., 2012; Biajoux et al., 2016).

Flow cytometric analyses

All staining analyses were performed on an LSRII Fortessa flow cytometer using the following mAbs: anti–mouse CD3 (clone 145-2C11, hamster IgG1), CD4 (clone RM4-5, rat IgG2a), CD8 (clone 53–6.7, rat IgG2a), CD11b (clone M1/70, rat IgG2b), CD16/32 (clone 93, rat IgG2a), CD21 (clone 7G6, rat IgG2b), CD25 (clone PC61, rat IgG1), CD34 (clone RAM34, rat IgG2a), CD41 (clone MWReg30, rat IgG1), CD43 (clone S7, rat IgG2a), CD44 (clone IM7, rat IgG2b), CD45R/B220 (clone RA3-6B2, rat IgG2a), CD45.1 (clone A20, mouse IgG2a), CD45.2 (clone 104, mouse IgG2a), CD48 (clone HM48-1, Armenian hamster IgG), CD62L (clone MEL-14, rat IgG2a), CD117 (clone 2B8, rat IgG2b), CD127 (clone A7R34, rat IgG2a), CD135 (clone A2F10, rat IgG2a), CD150 (clone TC15-23F12,2, rat IgG2a), Ter119 (clone TER-119, rat IgG2b), Gr-1 (clone RB6-8C5, rat IgG2b), Sca-1 (clone E13-161,7, rat IgG2a), IgM (clone II/41, ratIgG2a), and Cxcr4 (clone 2B11, rat IgG2b). Antibodies were conjugated to biotin, BV 650, FITC, PE, APC, AF700, PE-cyanin (Cy) 5, PE-Cy7, eFluor 450, AF 647, APC-eFluor 780, peridinin chlorophyll protein PerCP-Cy5,5, or pacific blue and purchased from BD, eBioscience, BioLegend, or Sony. The lineage antibody cocktail included anti-CD3, anti-CD45R, anti-CD11b, anti-TER119, anti-CD41, and anti–Gr-1 mAbs. Secondary labeling was performed with a Streptavidin–pacific orange from Thermo Fisher Scientific.

Immunofluorescence

Spleens were embedded in OCT medium (TissueTek). 7-µm cryosections were washed twice with PBS 1X and blocked in a solution of PBS BSA 5% for 1 h. Sections were stained overnight at 4°C and for 1 h at room temperature with the following unconjugated antibodies: polyclonal rabbit anti–mouse Cxcl12 (Thermo Fisher Scientific) and/or polyclonal goat anti–mouse Tcf21 (Santa Cruz Biotechnology, Inc.). Sections were washed twice with PBS 1X and incubated with the appropriate secondary antibody (Invitrogen): anti–rabbit and/or anti–goat conjugated to Alexa Fluor 594 or Alexa Fluor 488 for 30 min and 1 h, respectively, at room temperature together with DAPI for nuclear staining. Mounting was done using Permafluor mounting medium (Thermo Fisher Scientific). Slides were scanned using a NanoZoomer Digital Pathology system 40× objective lens with numerical aperture 0.75 (Hamamatsu Photonics).

ELISA

Spleens were harvested and cell suspensions were filtered through a 70-µm nylon strainer and centrifuged at 1,500 rpm for 5 min. The supernatants were collected and analyzed using a standardized ELISA for murine Cxcl12 (Quantikine; R&D Systems).

Quantitative real-time PCR

For *Cxcl12* expression, total cellular RNA was isolated from spleen cells using the RNeasy Plus Mini kit (QIAGEN) and

reverse transcribed with poly-d(T)-15 and Moloney murine leukemia virus reverse transcription (Fisher Bioblock). RNA was quantified using NanoDrop technology (Invitrogen). Amplification of cDNAs was performed by quantitative real-time PCR reactions on a Light Cycler instrument (LC480; Roche) with the LightCycler 480 SYBR Green detection kit (Roche) using the primers reported in Table S1. The dissociation curve method was applied according to the manufacturer's protocol (60°C to 95°C) to ensure the presence of a single specific PCR product. Relative quantification was performed with the standard curve method, and results were expressed as *Cxcl12/Gapdh* ratios. For *Cyclin* expression, purified BM ST-HSCs were frozen at −80°C during 5 min and then directly reverse transcribed with the SuperScript III Reverse transcriptase (Invitrogen). Amplification of cDNAs was performed by quantitative PCR reactions on a real-time PCR instrument (7500; Thermo Fisher Scientific Applied Biosystems) with the TaqMan Universal PCR Master Mix (Applied Biosystems) using the following primers (Applied Biosystems): *Ccnd1* (Mm00432359_m1), *Ccnd2* (Mm00438070_m1), *Ccnd3* (Mm01612362_m1), and *β-actin* (Mm01205647_g1). *β-actin* was used as the reference standard for normalization, and relative quantification of fold-differences in mRNA expression was determined by the comparative delta-delta-ct ($2^{-\Delta\Delta CT}$) method. Fold changes were calculated by setting the mean values obtained from WT cells as one.

Statistics

Data are expressed as mean ± SEM. All statistical analyses were conducted using Prism software (GraphPad Software). A Kruskal–Wallis test was used to determine the significance of the difference between means of WT, +/1013, and 1013/1013 groups ($^{\#}$, $P < 0.05$; $^{\#\#}$, $P < 0.005$; and $^{\#\#\#}$, $P < 0.0005$). The unpaired two-tailed Student *t* test (for mice experiments) or the Mann–Whitney test (for human experiments) was used to compare means among two groups.

Online supplemental material

Fig. S1 shows flow cytometric gating strategies for delineating mouse and human HSPCs. Table S1 lists the primers used for quantitative PCR (Lightcycler).

ACKNOWLEDGMENTS

We thank L. Quétier and M. Témagoult (INSERM UMR_S996, Clamart), Dr. H. Gary (IPS IT, Facility PLAIMMO, Clamart), P. Rameau and Y. Lecluse (Imaging and Cytometry Platform, IGR, Villejuif), B. Lecomte and M. Levant (IPSIT, Facility Animex, Clamart), as well as J.B. Lahaye and Dr. J. Bernardino-Sgherri (Plateforme d'Irradiation, CEA, Fontenay-Aux-Roses, France) for technical assistance. We are grateful to Dr. S. Flint (University of Cambridge, Cambridge, England, UK) for critical reading and editing of the manuscript.

The study was supported by Agence Nationale de la Recherche (ANR) grant 2010-JCJC-110401 to K. Balabanian. C. Freitas, J. Nguyen, V. Rondeau, V. Biajoux, F. Gaudin, F. Bachelerie, M. Espéli, A. Dalloul, and K. Balabanian are members of the LabEx LERMIT supported by ANR grant ANR-10-LABX-33 under the program "Investissements d'Avenir" ANR-11-IDEX-0003-01. This study was supported bythe Fondation de France (grant 2013 00038290) to F. Louache. C. Freitas was supported by DIM Biotherapies and the Société Française d'Hématologie. J. Nguyen was a PhD fellow from the DIM Cancéropôle. V. Rondeau was supported by the Fondation pour la Recherche Médicale (FRM, grant ECO20160736102). V. Biajoux was supported by fellowships from the French Ministry for Education and the FRM.

The authors declare no competing financial interests.

Author contributions: C. Freitas designed and performed most of the experiments and contributed to manuscript writing; M. Wittner, J. Nguyen, V. Rondeau, and V. Biajoux performed some of the experiments, analyzed data, and reviewed the manuscript; M.-L. Aknin and F. Gaudin performed some of the experiments and analyzed data; S. Beaussant-Cohen, Y. Bertrand, and J. Donadieu provided blood samples from healthy and patients with WS and reviewed the manuscript; C. Bellanné-Chantelot performed the genetic analyses and reviewed the manuscript; F. Bachelerie and M. Espéli reviewed the manuscript; A. Dalloul helped with the study design and contributed to data analyses; F. Louache designed and supervised the study, contributed to data analyses, found funding for the study, and wrote the manuscript. K. Balabanian conceived, designed, and supervised the study, contributed to data analyses, found funding for the study, and wrote the manuscript.

Submitted: 31 May 2016
Revised: 23 February 2017
Accepted: 19 April 2017

REFERENCES

Balabanian, K., B. Lagane, J.L. Pablos, L. Laurent, T. Planchenault, O. Verola, C. Lebbe, D. Kerob, A. Dupuy, O. Hermine, et al. 2005. WHIM syndromes with different genetic anomalies are accounted for by impaired CXCR4 desensitization to CXCL12. *Blood.* 105:2449–2457. http://dx.doi.org/10.1182/blood-2004-06-2289

Balabanian, K., A. Levoye, L. Klemm, B. Lagane, O. Hermine, J. Harriague, F. Baleux, F. Arenzana-Seisdedos, and F. Bachelerie. 2008. Leukocyte analysis from WHIM syndrome patients reveals a pivotal role for GRK3 in CXCR4 signaling. *J. Clin. Invest.* 118:1074–1084.

Balabanian, K., E. Brotin, V. Biajoux, L. Bouchet-Delbos, E. Lainey, O. Fenneteau, D. Bonnet, L. Fiette, D. Emilie, and F. Bachelerie. 2012. Proper desensitization of CXCR4 is required for lymphocyte development and peripheral compartmentalization in mice. *Blood.* 119:5722–5730. http://dx.doi.org/10.1182/blood-2012-01-403378

Baldridge, M.T., K.Y. King, N.C. Boles, D.C. Weksberg, and M.A. Goodell. 2010. Quiescent haematopoietic stem cells are activated by IFN-gamma in response to chronic infection. *Nature.* 465:793–797. http://dx.doi.org/10.1038/nature09135

Beaussant Cohen, S., O. Fenneteau, E. Plouvier, P.-S. Rohrlich, G. Daltroff, I. Plantier, A. Dupuy, D. Kerob, B. Beaupain, P. Bordigoni, et al. 2012. Description and outcome of a cohort of 8 patients with WHIM syndrome from the French Severe Chronic Neutropenia Registry. *Orphanet J. Rare Dis.* 7:71. http://dx.doi.org/10.1186/1750-1172-7-71

Biajoux, V., J. Natt, C. Freitas, N. Alouche, A. Sacquin, P. Hemon, F. Gaudin, N. Fazilleau, M. Espéli, and K. Balabanian. 2016. Efficient plasma cell differentiation and trafficking require Cxcr4 desensitization. *Cell Reports.* 17:193–205. http://dx.doi.org/10.1016/j.celrep.2016.08.068

Broxmeyer, H.E., C.M. Orschell, D.W. Clapp, G. Hangoc, S. Cooper, P.A. Plett, W.C. Liles, X. Li, B. Graham-Evans, T.B. Campbell, et al. 2005. Rapid mobilization of murine and human hematopoietic stem and progenitor cells with AMD3100, a CXCR4 antagonist. *J. Exp. Med.* 201:1307–1318. http://dx.doi.org/10.1084/jem.20041385

Cho, S.K., T.D. Webber, J.R. Carlyle, T. Nakano, S.M. Lewis, and J.C. Zúñiga-Pflücker. 1999. Functional characterization of B lymphocytes generated in vitro from embryonic stem cells. *Proc. Natl. Acad. Sci. USA.* 96:9797–9802. http://dx.doi.org/10.1073/pnas.96.17.9797

Christopher, M.J., F. Liu, M.J. Hilton, F. Long, and D.C. Link. 2009. Suppression of CXCL12 production by bone marrow osteoblasts is a common and critical pathway for cytokine-induced mobilization. *Blood.* 114:1331–1339. http://dx.doi.org/10.1182/blood-2008-10-184754

Cordeiro Gomes, A., T. Hara, V.Y. Lim, D. Herndler-Brandstetter, E. Nevius, T. Sugiyama, S. Tani-Ichi, S. Schlenner, E. Richie, H.-R. Rodewald, et al. 2016. Hematopoietic stem cell niches produce lineage-instructive signals to control multipotent progenitor differentiation. *Immunity.* 45:1219–1231. http://dx.doi.org/10.1016/j.immuni.2016.11.004

Ding, L., and S.J. Morrison. 2013. Haematopoietic stem cells and early lymphoid progenitors occupy distinct bone marrow niches. *Nature.* 495:231–235. http://dx.doi.org/10.1038/nature11885

Dotta, L., L. Tassone, and R. Badolato. 2011. Clinical and genetic features of warts, hypogammaglobulinemia, infections and myelokathexis (WHIM) syndrome. *Curr. Mol. Med.* 11:317–325. http://dx.doi.org/10.2174/156652411795677963

Doulatov, S., F. Notta, E. Laurenti, and J.E. Dick. 2012. Hematopoiesis: A human perspective. *Cell Stem Cell.* 10:120–136. http://dx.doi.org/10.1016/j.stem.2012.01.006

Eash, K.J., A.M. Greenbaum, P.K. Gopalan, and D.C. Link. 2010. CXCR2 and CXCR4 antagonistically regulate neutrophil trafficking from murine bone marrow. *J. Clin. Invest.* 120:2423–2431. http://dx.doi.org/10.1172/JCI41649

Foudi, A., P. Jarrier, Y. Zhang, M. Wittner, J.-F. Geay, Y. Lecluse, T. Nagasawa, W. Vainchenker, and F. Louache. 2006. Reduced retention of radioprotective hematopoietic cells within the bone marrow microenvironment in CXCR4$^{-/-}$ chimeric mice. *Blood.* 107:2243–2251. http://dx.doi.org/10.1182/blood-2005-02-0581

Galloway, A., A. Saveliev, S. Łukasiak, D.J. Hodson, D. Bolland, K. Balmanno, H. Ahlfors, E. Monzón-Casanova, S.C. Mannurita, L.S. Bell, et al. 2016. RNA-binding proteins ZFP36L1 and ZFP36L2 promote cell quiescence. *Science.* 352:453–459. http://dx.doi.org/10.1126/science.aad5978

Gautreau, L., A. Boudil, V. Pasqualetto, L. Skhiri, L. Grandin, M. Monteiro, J.-P. Jais, and S. Ezine. 2010. Gene coexpression analysis in single cells indicates lymphomyeloid copriming in short-term hematopoietic stem cells and multipotent progenitors. *J. Immunol. Baltim. Md.* 184:4907–4917.

Gulino, A.V., D. Moratto, S. Sozzani, P. Cavadini, K. Otero, L. Tassone, L. Imberti, S. Pirovano, L.D. Notarangelo, R. Soresina, et al. 2004. Altered leukocyte response to CXCL12 in patients with warts hypogammaglobulinemia, infections, myelokathexis (WHIM) syndrome. *Blood.* 104:444–452. http://dx.doi.org/10.1182/blood-2003-10-3532

Hernandez, P.A., R.J. Gorlin, J.N. Lukens, S. Taniuchi, J. Bohinjec, F. Francois, M.E. Klotman, and G.A. Diaz. 2003. Mutations in the chemokine receptor gene CXCR4 are associated with WHIM syndrome, a combined immunodeficiency disease. *Nat. Genet.* 34:70–74. http://dx.doi.org/10.1038/ng1149

Hidalgo, I., A. Herrera-Merchan, J.M. Ligos, L. Carramolino, J. Nuñez, F. Martinez, O. Dominguez, M. Torres, and S. Gonzalez. 2012. Ezh1 is required for hematopoietic stem cell maintenance and prevents senescence-like cell cycle arrest. *Cell Stem Cell.* 11:649–662. http://dx.doi.org/10.1016/j.stem.2012.08.001

Inra, C.N., B.O. Zhou, M. Acar, M.M. Murphy, J. Richardson, Z. Zhao, and S.J. Morrison. 2015. A perisinusoidal niche for extramedullary haematopoiesis in the spleen. *Nature.* 527:466–471. http://dx.doi.org/10.1038/nature15530

Itkin, T., S. Gur-Cohen, J.A. Spencer, A. Schajnovitz, S.K. Ramasamy, A.P. Kusumbe, G. Ledergor, Y. Jung, I. Milo, M.G. Poulos, et al. 2016. Distinct bone marrow blood vessels differentially regulate haematopoiesis. *Nature.* 532:323–328. http://dx.doi.org/10.1038/nature17624

Ito, K., A. Hirao, F. Arai, K. Takubo, S. Matsuoka, K. Miyamoto, M. Ohmura, K. Naka, K. Hosokawa, Y. Ikeda, and T. Suda. 2006. Reactive oxygen species act through p38 MAPK to limit the lifespan of hematopoietic stem cells. *Nat. Med.* 12:446–451. http://dx.doi.org/10.1038/nm1388

Karpova, D., and H. Bonig. 2015. Concise Review: CXCR4/CXCL12 signaling in immature hematopoiesis—Lessons from pharmacological and genetic models. *Stem Cells.* 33:2391–2399. http://dx.doi.org/10.1002/stem.2054

Kawabata, K., M. Ujikawa, T. Egawa, H. Kawamoto, K. Tachibana, H. Iizasa, Y. Katsura, T. Kishimoto, and T. Nagasawa. 1999. A cell-autonomous requirement for CXCR4 in long-term lymphoid and myeloid reconstitution. *Proc. Natl. Acad. Sci. USA.* 96:5663–5667. http://dx.doi.org/10.1073/pnas.96.10.5663

Kawai, T., and H.L. Malech. 2009. WHIM syndrome: Congenital immune deficiency disease. *Curr. Opin. Hematol.* 16:20–26. http://dx.doi.org/10.1097/MOH.0b013e32831ac557

Kawai, T., U. Choi, L. Cardwell, S.S. DeRavin, N. Naumann, N.L. Whiting-Theobald, G.F. Linton, J. Moon, P.M. Murphy, and H.L. Malech. 2007. WHIM syndrome myelokathexis reproduced in the NOD/SCID mouse xenotransplant model engrafted with healthy human stem cells transduced with C-terminus-truncated CXCR4. *Blood.* 109:78–84. http://dx.doi.org/10.1182/blood-2006-05-025296

Kozar, K., M.A. Ciemerych, V.I. Rebel, H. Shigematsu, A. Zagozdzon, E. Sicinska, Y. Geng, Q. Yu, S. Bhattacharya, R.T. Bronson, et al. 2004. Mouse development and cell proliferation in the absence of D-cyclins. *Cell.* 118:477–491. http://dx.doi.org/10.1016/j.cell.2004.07.025

Kriván, G., M. Erdos, K. Kállay, G. Benyó, A. Tóth, J. Sinkó, V. Goda, B. Tóth, and L. Maródi. 2010. Successful umbilical cord blood stem cell transplantation in a child with WHIM syndrome. *Eur. J. Haematol.* 84:274–275. http://dx.doi.org/10.1111/j.1600-0609.2009.01368.x

Lai, C.-Y., S. Yamazaki, M. Okabe, S. Suzuki, Y. Maeyama, Y. Iimura, M. Onodera, S. Kakuta, Y. Iwakura, M. Nojima, et al. 2014. Stage-specific roles for CXCR4 signaling in murine hematopoietic stem/progenitor cells in the process of bone marrow repopulation. *Stem Cells.* 32:1929–1942. http://dx.doi.org/10.1002/stem.1670

Ma, Q., D. Jones, P.R. Borghesani, R.A. Segal, T. Nagasawa, T. Kishimoto, R.T. Bronson, and T.A. Springer. 1998. Impaired B-lymphopoiesis, myelopoiesis, and derailed cerebellar neuron migration in CXCR4- and SDF-1-deficient mice. *Proc. Natl. Acad. Sci. USA.* 95:9448–9453. http://dx.doi.org/10.1073/pnas.95.16.9448

McDermott, D.H., J.-L. Gao, Q. Liu, M. Siwicki, C. Martens, P. Jacobs, D. Velez, E. Yim, C.R. Bryke, N. Hsu, et al. 2015. Chromothriptic cure of WHIM syndrome. *Cell.* 160:686–699. http://dx.doi.org/10.1016/j.cell.2015.01.014

Miwa, Y., T. Hayashi, S. Suzuki, S. Abe, I. Onishi, S. Kirimura, M. Kitagawa, and M. Kurata. 2013. Up-regulated expression of CXCL12 in human spleens with extramedullary haematopoiesis. *Pathology.* 45:408–416. http://dx.doi.org/10.1097/PAT.0b013e3283613dbf

Morrison, S.J., D.E. Wright, and I.L. Weissman. 1997. Cyclophosphamide/granulocyte colony-stimulating factor induces hematopoietic stem cells to proliferate prior to mobilization. *Proc. Natl. Acad. Sci. USA.* 94:1908–1913. http://dx.doi.org/10.1073/pnas.94.5.1908

Nagasawa, T., S. Hirota, K. Tachibana, N. Takakura, S. Nishikawa, Y. Kitamura, N. Yoshida, H. Kikutani, and T. Kishimoto. 1996. Defects of B-cell lymphopoiesis and bone-marrow myelopoiesis in mice lacking the CXC chemokine PBSF/SDF-1. *Nature.* 382:635–638. http://dx.doi.org/10.1038/382635a0

Nagasawa, T., K. Tachibana, and T. Kishimoto. 1998. A novel CXC chemokine PBSF/SDF-1 and its receptor CXCR4: their functions in development, hematopoiesis and HIV infection. *Semin. Immunol.* 10:179–185. http://dx.doi.org/10.1006/smim.1998.0128

Nie, Y., Y.-C. Han, and Y.-R. Zou. 2008. CXCR4 is required for the quiescence of primitive hematopoietic cells. *J. Exp. Med.* 205:777–783. http://dx.doi.org/10.1084/jem.20072513

Onai, N., Yy. Zhang, H. Yoneyama, T. Kitamura, S. Ishikawa, and K. Matsushima. 2000. Impairment of lymphopoiesis and myelopoiesis in mice reconstituted with bone marrow-hematopoietic progenitor cells expressing SDF-1-intrakine. *Blood.* 96:2074–2080.

Orford, K.W., and D.T. Scadden. 2008. Deconstructing stem cell self-renewal: Genetic insights into cell-cycle regulation. *Nat. Rev. Genet.* 9:115–128. http://dx.doi.org/10.1038/nrg2269

Peled, A., I. Petit, O. Kollet, M. Magid, T. Ponomaryov, T. Byk, A. Nagler, H. Ben-Hur, A. Many, L. Shultz, et al. 1999. Dependence of human stem cell engraftment and repopulation of NOD/SCID mice on CXCR4. *Science.* 283:845–848. http://dx.doi.org/10.1126/science.283.5403.845

Pitt, L.A., A.N. Tikhonova, H. Hu, T. Trimarchi, B. King, Y. Gong, M. Sanchez-Martin, A. Tsirigos, D.R. Littman, A.A. Ferrando, et al. 2015. CXCL12-producing vascular endothelial niches control acute T cell leukemia maintenance. *Cancer Cell.* 27:755–768. http://dx.doi.org/10.1016/j.ccell.2015.05.002

Scimone, M.L., T.W. Felbinger, I.B. Mazo, J.V. Stein, U.H. Von Andrian, and W. Weninger. 2004. CXCL12 mediates CCR7-independent homing of central memory cells, but not naive T cells, in peripheral lymph nodes. *J. Exp. Med.* 199:1113–1120. http://dx.doi.org/10.1084/jem.20031645

Shao, L., H. Li, S.K. Pazhanisamy, A. Meng, Y. Wang, and D. Zhou. 2011. Reactive oxygen species and hematopoietic stem cell senescence. *Int. J. Hematol.* 94:24–32. http://dx.doi.org/10.1007/s12185-011-0872-1

Sugiyama, T., H. Kohara, M. Noda, and T. Nagasawa. 2006. Maintenance of the hematopoietic stem cell pool by CXCL12-CXCR4 chemokine signaling in bone marrow stromal cell niches. *Immunity.* 25:977–988. http://dx.doi.org/10.1016/j.immuni.2006.10.016

Trampont, P.C., A.-C. Tosello-Trampont, Y. Shen, A.K. Duley, A.E. Sutherland, T.P. Bender, D.R. Littman, and K.S. Ravichandran. 2010. CXCR4 acts as a costimulator during thymic beta-selection. *Nat. Immunol.* 11:162–170. http://dx.doi.org/10.1038/ni.1830

Tsai, J.J., J.A. Dudakov, K. Takahashi, J.-H. Shieh, E. Velardi, A.M. Holland, N.V. Singer, M.L. West, O.M. Smith, L.F. Young, et al. 2013. Nrf2 regulates haematopoietic stem cell function. *Nat. Cell Biol.* 15:309–316. http://dx.doi.org/10.1038/ncb2699

Tzeng, Y.-S., H. Li, Y.-L. Kang, W.-C. Chen, W.-C. Cheng, and D.-M. Lai. 2011. Loss of Cxcl12/Sdf-1 in adult mice decreases the quiescent state of hematopoietic stem/progenitor cells and alters the pattern of hematopoietic regeneration after myelosuppression. *Blood.* 117:429–439. http://dx.doi.org/10.1182/blood-2010-01-266833

Wang, X., S.Y. Cho, C.S. Hu, D. Chen, J. Roboz, and R. Hoffman. 2015. C-X-C motif chemokine 12 influences the development of extramedullary hematopoiesis in the spleens of myelofibrosis patients. *Exp. Hematol.* 43:100–109.e1. http://dx.doi.org/10.1016/j.exphem.2014.10.013

Wilson, A., E. Laurenti, G. Oser, R.C. van der Wath, W. Blanco-Bose, M. Jaworski, S. Offner, C.F. Dunant, L. Eshkind, E. Bockamp, et al. 2008. Hematopoietic stem cells reversibly switch from dormancy to self-renewal during homeostasis and repair. *Cell.* 135:1118–1129. http://dx.doi.org/10.1016/j.cell.2008.10.048

Wolf, B.C., and R.S. Neiman. 1987. Hypothesis: splenic filtration and the pathogenesis of extramedullary hematopoiesis in agnogenic myeloid metaplasia. *Hematol. Pathol.* 1:77–80.

Yahata, T., T. Takanashi, Y. Muguruma, A.A. Ibrahim, H. Matsuzawa, T. Uno, Y. Sheng, M. Onizuka, M. Ito, S. Kato, and K. Ando. 2011. Accumulation of oxidative DNA damage restricts the self-renewal capacity of human hematopoietic stem cells. *Blood.* 118:2941–2950. http://dx.doi.org/10.1182/blood-2011-01-330050

Young, K., S. Borikar, R. Bell, L. Kuffler, V. Philip, and J.J. Trowbridge. 2016. Progressive alterations in multipotent hematopoietic progenitors underlie lymphoid cell loss in aging. *J. Exp. Med.* 213:2259–2267. http://dx.doi.org/10.1084/jem.20160168

Zhang, Y., A. Foudi, J.-F. Geay, M. Berthebaud, D. Buet, P. Jarrier, A. Jalil, W. Vainchenker, and F. Louache. 2004. Intracellular localization and constitutive endocytosis of CXCR4 in human CD34+ hematopoietic progenitor cells. *Stem Cells.* 22:1015–1029. http://dx.doi.org/10.1634/stemcells.22-6-1015

Zhang, Y., M. Dépond, L. He, A. Foudi, E.O. Kwarteng, E. Lauret, I. Plo, C. Desterke, P. Dessen, N. Fujii, et al. 2016. CXCR4/CXCL12 axis counteracts hematopoietic stem cell exhaustion through selective protection against oxidative stress. *Sci. Rep.* 6:37827. http://dx.doi.org/10.1038/srep37827